AD-A078 644 NATIONAL AERONAUTICS AND SPACE ADMINISTRATION HAMPTO--ETC F/G 20/4
EFFECTS OF FUSELAGE FOREBODY GEOMETRY ON LOW-SPEED LATERAL-DIRE--ETC(U)
DEC 79 P C CARR , W P GILBERT

UNCLASSIFIED NASA-L-13270 NASA -TP-1592 NL

| OF |
AD
A078644

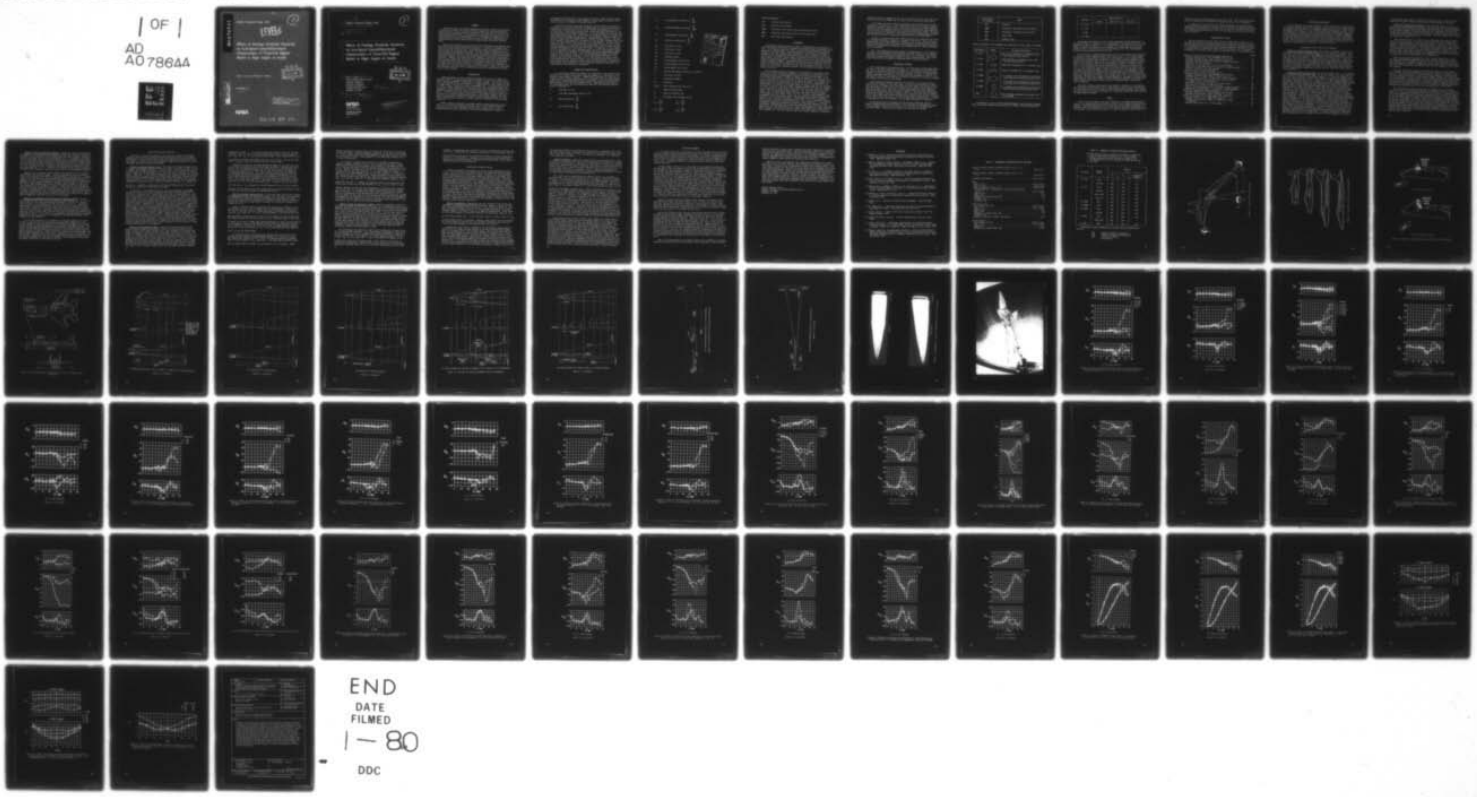

END
DATE
FILMED
1 — 80
DDC

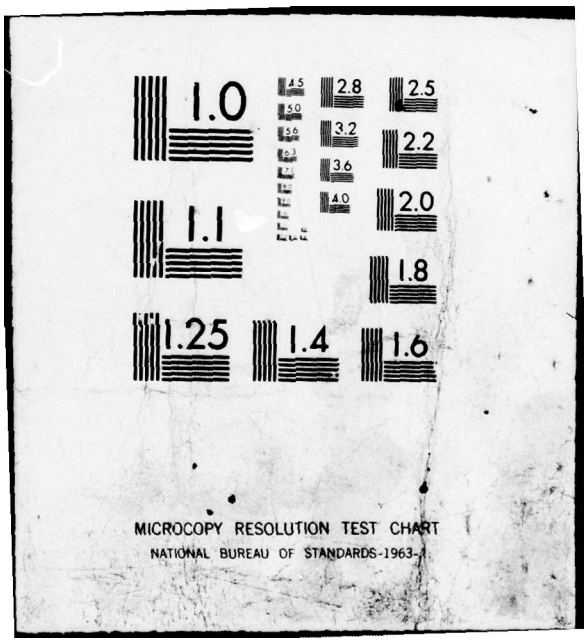
1.0
1.1
1.25
1.4
1.6
1.8
2.0
2.2
2.5
2.8
3.2
3.6
4.0
4.5
5.0
5.6
MICROCOPY RESOLUTION TEST CHART
NATIONAL BUREAU OF STANDARDS-1963-A

ADA078644

NASA Technical Paper 1592

LEVEL II

Effects of Fuselage Forebody Geometry on Low-Speed Lateral-Directional Characteristics of Twin-Tail Fighter Model at High Angles of Attack

DDC RECEIVED DEC 28 1979 E

Peter C. Carr and William P. Gilbert

DDC FILE COPY

DECEMBER 1979

This document has been approved for public release and sale; its distribution is unlimited.

NASA

79-12 27 105

(18) NASA (9) Technical Paper, 1592

(19) TP-1592

(1)

(6) # Effects of Fuselage Forebody Geometry on Low-Speed Lateral-Directional Characteristics of Twin-Tail Fighter Model at High Angles of Attack.

DDC
RECEIVED
DEC 28 1979
E

(10) Peter C. Carr
Dryden Flight Research Center
Edwards, California

William P. Gilbert
Langley Research Center
Hampton, Virginia

(14) NASA-L-13270

(11) Dec 79 (12) 73

NASA
National Aeronautics
and Space Administration

**Scientific and Technical
Information Branch**

1979

This document has been approved for public release and sale; its distribution is unlimited.

387 543

out

SUMMARY

Wind-tunnel tests have been conducted with a modern fighter configuration to explore the effects of fuselage forebody geometry on lateral-directional characteristics at high angles of attack and to provide data for formulating general design procedures. The investigation consisted of low-speed, static, wind-tunnel tests of a fighter model over a large angle-of-attack range with eight different forebody configurations; also included was consideration of forebody devices such as nose strakes, boundary-layer trip wires, and nose booms.

Results were obtained in the areas of lateral-directional aerodynamic symmetry and stability and longitudinal stability. In general, forebody design features such as fineness ratio, cross-sectional shape, and devices like forebody strakes and nose booms had a large influence on both lateral-directional and longitudinal aerodynamic stability. For the airplane configuration tested, results showed that several of the forebodies produced both lateral-directional aerodynamic symmetry and strong favorable changes in directional and lateral stability. However, the same results also indicated that such forebody designs could produce significant reductions in longitudinal stability near maximum lift and could significantly change the influence which other configuration variables have on airplane stability. Furthermore, these tests indicated that the addition of devices such as flight-test nose booms to highly tailored forebody designs could significantly degrade the stability improvements provided by the clean forebody.

INTRODUCTION

High performance military airplanes designed for air-to-air combat are normally flown at extremely high angles of attack to obtain the turning performance required to maneuver effectively at subsonic speeds. The values of angle of attack reached during such vigorous air combat maneuvers often approach, and at times exceed, the angle of attack for maximum lift. At such extreme angles of attack, fighter configurations may experience large aerodynamic asymmetries, along with a severe degradation in stability and control characteristics; these degraded characteristics can result in inadvertent loss of control and spin entry. In view of the relative importance of high angle-of-attack flight characteristics for highly maneuverable aircraft, considerable emphasis has been placed on developing airframe and automatic-control-system concepts which provide a high degree of stability, control, and spin resistance for such flight conditions.

Recent research conducted by the NASA Langley and Ames Research Centers (refs. 1 to 6) and by airframe contractors (ref. 7) has indicated that the relatively long, pointed fuselage forebody used for many current fighter configurations can have significant, and sometimes predominant, effects on

aerodynamic characteristics at high angles of attack. These effects include the generation of extremely large asymmetric yawing moments and large variations in static and dynamic directional stability.

The present investigation was conducted to further explore the effects of geometric variations of fuselage forebody shape on lateral-directional and longitudinal characteristics for a current fighter configuration with twin vertical tails. The primary objective was to provide additional data for use in formulating general design procedures. The investigation consisted of low-speed wind-tunnel tests over a large range of angles of attack for a model with eight different forebody configurations. The forebodies tested included six different cross-sectional shapes and two forebody fineness ratios. The tests also included an evaluation of the effects of nose strakes, boundary-layer trip wires, and nose booms affixed to several of the forebodies. Previous investigations (refs. 1 to 7) have shown that such add-on devices as nose strakes and nose booms (for flight-test air-data measurements) can strongly influence forebody aerodynamics at high angles of attack. In addition, a recent paper (ref. 8) has shown that small boundary-layer trip wires, when properly placed on the forebody, can suppress the development of large yawing-moment asymmetries at high angles of attack. The two aerodynamic parameters of primary interest in the present study were (1) the yawing moment measured at zero sideslip and high angles of attack, and (2) the variation of static directional stability with angle of attack. All the lateral-directional results are presented herein, together with selected longitudinal data. Results of a water-tunnel flow visualization study, which was conducted to parallel this investigation, are presented in reference 9.

SYMBOLS AND ABBREVIATIONS

All longitudinal forces and moments are referenced to the stability-axis system and all lateral-directional forces and moments are referenced to the body-axis system shown in figure 1. Moment data presented are referenced to a moment center located longitudinally at 26 percent of the wing mean aerodynamic chord. Dimensional quantities are presented in both the International System of Units (SI) and U.S. Customary Units. Measurements were made in U.S. Customary Units, and conversions were made with the conversion factors given in reference 10.

b wing span, m (ft)

$\bar{c}$ wing mean aerodynamic chord, m (ft)

C_D drag coefficient, $\frac{F_D}{\bar{q}S}$

C_L lift coefficient, $\frac{F_L}{\bar{q}S}$

C_l rolling-moment coefficient, $\frac{M_X}{\bar{q}Sb}$

C_m pitching-moment coefficient, $\frac{M_Y}{\bar{q}S\bar{c}}$

C_n yawing-moment coefficient, $\frac{M_Z}{\bar{q}Sb}$

C_Y side-force coefficient, $\frac{F_Y}{qS}$

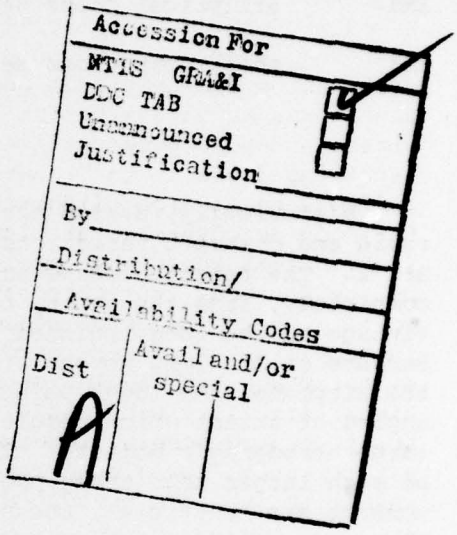

F_D drag force, N (lb)

F_L lift force, N (lb)

F_Y side force, N (lb)

FS fuselage station

M_X rolling moment, N-m (ft-lb)

M_Y pitching moment, N-m (ft-lb)

M_Z yawing moment, N-m (ft-lb)

$\bar{q}$ free-stream dynamic pressure, Pa (lb/ft^2)

S wing area, m^2 (ft^2)

V resultant airspeed

WL waterline

X,Y,Z body reference axes (see fig. 1)

α angle of attack, deg

β angle of sideslip, deg

δ_h horizontal tail deflection, deg

$C_{l_\beta} = \frac{\partial C_l}{\partial \beta}$ $\quad C_{Y_\beta} = \frac{\partial C_Y}{\partial \beta}$

$C_{n_\beta} = \frac{\partial C_n}{\partial \beta}$ $\quad C_{m_\alpha} = \frac{\partial C_m}{\partial \alpha}$

Model designations:

CIR	circular cross section
DKB	duckbill cross section
EMAH	elliptical cross section with horizontal major axis
EMAV	elliptical cross section with vertical major axis
SHK	shark nose cross section

BACKGROUND

Historically, design trends for fighter configurations have resulted in rapid and dramatic variations in geometric airframe designs as depicted in figure 2. The relative shape and length of the fuselage forebody have changed completely, from the short, blunt-nose geometry of fighters of World War II vintage to the long, pointed noses employed in current supersonic fighters. Because of the long moment arm between the nose and the center of gravity of the airplane, the long, pointed nose can generate strong vortex flows at high angles of attack which result in differential forces on the nose and extremely large aerodynamic moments. The moments produced by the fuselage forebody can be much larger than those produced by the tail and control surfaces. If the moments are beneficial, the stability and control characteristics of the airplane are significantly enhanced; however, if the moments are adverse, loss of control may occur.

The aerodynamic effects produced by the forebody are of interest under conditions of zero and nonzero sideslip. As discussed in references 2 to 7, the large asymmetric yawing moments produced by long, pointed noses are of considerable importance to studies of departure and spin. As shown in figure 3, flow separation on a long nose at zero sideslip tends to produce a symmetrical pattern of vortex sheets at low angles of attack. This symmetrical flow pattern does not produce any side force on the nose; consequently, no yawing moment is produced. At higher angles of attack, however, the vortices increase in strength; the flow pattern becomes asymmetrical; and the asymmetrical flow produces a side force on the nose which, in turn, produces a yawing moment about the airplane center of gravity. For extremely high angles of attack, such as those angles associated with post-stall flight and spins, these shapes have been found (refs. 2 and 7) to produce large asymmetric yawing moments which can be much larger than the corrective moments produced by deflection of a conventional rudder. These moments may have a predominant effect on stall and spin characteristics and can, in fact, determine the ease and direction in which an airplane may spin. (See reference 2.) Although the aerodynamic asymmetries produced by sharp noses have been measured in past wind-tunnel investigations of airplane spin characteristics, the basic flow phenomena were not well understood. As a result, the asymmetries either have often been ignored or have been attributed to poor wind-tunnel flow or significant model asymmetries. The more recent flight test results reported in reference 7

indicated that such asymmetries exist for full-scale aircraft and flight conditions and that the asymmetries can cause loss of control and spin entry.

With regard to nonzero sideslip conditions, past studies such as those discussed in references 2, 5, and 7 have shown that certain fuselage forebody designs can produce a high level of directional stability, and that geometric variables such as forebody fineness ratio and cross-sectional shape apparently can be used to take advantage of this potentially beneficial effect. Moreover, results presented in reference 7 also point out that forebody geometry changes may substantially effect longitudinal characteristics (pitching moment).

In order to derive quantitative design information on desirable and feasible fuselage forebodies, research is required in two areas. First, the aerodynamic effect of forebody geometric variables such as cross-sectional shape, nose fineness ratio, and nose probes and booms must be determined; second, the effects of aerodynamically beneficial nose-radome-shapes on radar performance must be assessed.

The primary objectives of the present investigation were (1) to explore the beneficial aerodynamic effects produced by proper shaping of the fuselage forebody of a current fighter configuration and (2) to correlate the results with those obtained during past studies of other configurations. Thus, additional data would be provided to formulate general design procedures.

DESCRIPTION OF MODEL

The investigation was conducted with a 0.10-scale free-flight model which was used in the tests reported in reference 11. The model was refurbished for the current testing and modified to accept several different fuselage forebody designs. A three-view sketch of the model is shown in figure 4, and some pertinent dimensional characteristics of the model are presented in table I. As indicated in figure 4, the parting line used for mounting the various forebodies was located just forward of the canopy.

Eight different fuselage forebodies were tested in this investigation, including the forebody of the basic model. The various forebodies are identified in terms of fineness ratio and cross-sectional shape. The fineness ratio definition used in this study was the ratio of the forebody length (measured from the parting line to the tip) to the forebody depth (vertical dimension measured at the parting line) as shown in figure 4. Note that several methods of defining fineness ratio have evolved in the literature and that the method used in this report may differ from definitions used in other studies. Fineness ratios used in these tests were 2.3 for the basic model forebody and 3.5, which is representative of the forebody of the airplane discussed in reference 7.

To facilitate ease of discussion of the various forebodies tested, a simple designation has been assigned for each forebody; the designation refers to the forebody fineness ratio (either 2.3 or 3.5) and the forebody cross-sectional shape. Cross-sectional shapes are identified as follows:

Abbreviation or acronym	Shape
CIR	Circular
EMAH	Elliptical, with major axis horizontal
EMAV	Elliptical, with major axis vertical
SHK	Shark nose
DKB	Duckbill nose

Using this scheme, the forebodies are referred to in this report as follows:

Designation	Shape	Forebody description
2.3 CIR	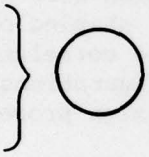	Basic short forebody (2.3 fineness ratio) with circular cross section
3.5 CIR		Long forebody (3.5 fineness ratio) with circular cross section
3.5 SHK		Shark-nose forebody with 3.5 fineness ratio
3.5 DKB		Duckbill forebody with 3.5 fineness ratio
2.3 EMAH	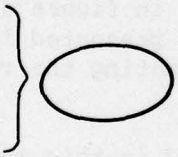	2.3 fineness ratio forebody with elliptical cross section with horizontal major axis
3.5 EMAH		3.5 fineness ratio forebody with elliptical cross section with horizontal major axis
3.5 EMAV		3.5 fineness ratio forebody with elliptical cross section with vertical major axis
Blunt		Blunt forebody representing fuselage without forebody

In addition to tests of these forebody shapes, the study also included tests of several forebody add-on devices as listed in the following table:

Forebody	Add-on device		
	Strake	Nose boom	Trip wire
2.3 CIR	✓		
3.5 CIR	✓	✓	✓
3.5 DKB		✓	
3.5 EMAV	✓		

Photographs and sketches of the various forebodies and forebody add-on devices are shown in figures 5 to 9; a photograph of the model with the 3.5 DKB forebody is shown in figure 10. It is important to note that the trip wire shown in figure 9 is mounted on the forebody in a unique fashion and is most effective only if mounted in such a helical pattern (ref. 8). The diameter of the wire tested was 0.318 cm (0.125 in.).

The particular forebody shapes chosen for this investigation were selected on the basis of past experience and a few studies (refs. 1 to 7) which appear to indicate trends produced by families of nose shapes. The elliptical cross section with the major axis oriented in a horizontal direction (EMAH) has been found in past studies (refs. 2 and 5) to produce significant beneficial contributions to directional stability at high angles of attack. A similar study (ref. 1) has indicated that severe degradations in directional stability can result if the elliptical cross section is oriented such that the major axis is in a vertical direction (EMAV). Recent tests (ref. 6) of a supersonic cruise transport configuration indicated that the same duckbill DKB forebody as that used in the present study produced an extremely high level of directional stability at high angles of attack. Also, flight tests (ref. 7) of the shark nose SHK shape indicated that asymmetric yawing moments at high angles of attack were suppressed and directional stability was dramatically improved. The blunt nose was included in the current tests in order to determine model aerodynamics with no forebody.

The add-on devices noted earlier were tested to evaluate (1) the effects of flight-test installations, such as nose booms, on the relative contributions of the forebodies, and (2) the use of fixed installations, such as nose strakes and the helical trip wire of reference 8, to eliminate undesirable contributions of nonoptimum nose shapes.

TESTS

Static force and moment tests were conducted at the NASA Langley Research Center in a low-speed wind tunnel with a 3.66-m (12-ft) diameter octagonal test section. The data presented in this report were derived from tests made at a Reynolds number of approximately 0.59×10^6 based on the mean aerodynamic chord of the wing. Static tests were made for a range of angles of attack from 0° to

55° over a range of sideslip angles from -20° to 20°. The lateral-directional stability derivatives were based on sloping data from -5° to 5° sideslip.

In addition to the tests of the fuselage forebodies and forebody add-on devices previously described, the model was tested with the engine inlet cowls undeflected and deflected to 12° down (fig. 4), with the all-moving horizontal tail undeflected and deflected to 25° trailing edge up, and with the vertical tails on and off.

PRESENTATION OF DATA

The data obtained from the force tests are presented in figures 11 to 31 and show the effects of forebody fineness ratio, cross section, and selected forebody add-on devices on lateral-directional aerodynamic symmetry and stability. Although the lateral-directional characteristics are of primary interest, a limited amount of longitudinal data are also presented. For the reader's convenience, an outline of the content of the data figures is presented below:

	Figure
Effect on lateral-directional aerodynamic symmetry of -	
Forebody fineness ratio (CIR and EMAH cross sections)	11
Forebody cross-sectional shape (fineness ratio 3.5)	12
Fuselage forebody strakes (3.5 CIR and 3.5 EMAV forebodies)	13
Nose boom (3.5 CIR forebody)	14
Boundary-layer helical trip wire (3.5 CIR forebody)	15
Engine inlet cowl deflection (3.5 CIR and 3.5 DKB forebodies)	16
Elevator deflection (3.5 CIR forebody)	17
Vertical tails (3.5 CIR forebody)	18
Effect on lateral-directional stability of -	
Forebody fineness ratio (CIR and EMAH cross sections)	19
Forebody cross-sectional shape (fineness ratio 3.5)	20
Vertical tails (3.5 CIR, 3.5 SHK, and 3.5 DKB forebodies)	21
Fuselage forebody strakes and vertical tails (3.5 CIR, 3.5 EMAV, and 2.3 CIR forebodies)	22
Boundary-layer helical trip wire (3.5 CIR forebody)	23
Nose boom (3.5 CIR and 3.5 DKB forebodies)	24
Engine inlet cowl deflection (3.5 CIR and 3.5 DKB forebodies)	25
Horizontal-tail deflection (3.5 CIR and 3.5 DKB forebodies)	26
Effect on longitudinal characteristics at $\beta = 0°$ of -	
Forebody fineness ratio (CIR and EMAH cross sections)	27
Forebody cross-sectional shape (fineness ratio 3.5)	28
Effect on variation of pitching moment with sideslip of -	
Forebody fineness ratio (EMAH cross section)	29
Forebody cross-sectional shape (3.5 EMAV and 3.5 DKB forebodies)	30
Forebody add-on devices (3.5 CIR forebody)	31

RESULTS AND DISCUSSION

As was expected, the results obtained in this investigation indicate that the fuselage forebody design had a dominant influence on the lateral-directional aerodynamic characteristics of the complete model configuration. These results are summarized in table II. The effects observed are discussed herein to show the influence of forebody design on lateral-directional aerodynamic symmetry, lateral-directional stability, and longitudinal stability. Data are presented to show the effects of forebody fineness ratio and cross section; the effects of nose strakes, nose helical trip wires, and nose booms; and the influence of several other configuration variables of the basic model, including inlet cowl deflection, horizontal-tail deflection, and vertical tails.

Aerodynamic Lateral-Directional Symmetry

Effect of forebody fineness ratio.- The effect of forebody fineness ratio on lateral-directional aerodynamic symmetry at zero sideslip is shown in figures 11(a) and 11(b) for the CIR and EMAH cross sections, respectively. The data show that large asymmetric yawing moments are produced by the circular and elliptical cross sections for a fineness ratio of 3.5 above 35° α and that the moments are much larger than those which could be produced by rudder inputs at high angles of attack. The asymmetric yawing moments for the forebodies with the 2.3 fineness ratio were much smaller. These results tend to confirm the results of other investigations (refs. 3 and 4) which have shown that significant yawing-moment asymmetries develop only for relatively high-fineness-ratio forebodies.

Effect of cross-sectional shape.- The results showed (fig. 11) that changes to the forebody cross-sectional shape for the low fineness ratio were found to have little or no effect on aerodynamic symmetry. In contrast, forebody cross-sectional shape was found to have a significant influence on aerodynamic symmetry for a fineness ratio of 3.5. (See fig. 12.) The largest asymmetric yawing moments were exhibited by the forebodies having CIR and EMAH cross-sectional shapes. Much smaller asymmetries were measured on the more unusual SHK and DKB forebodies. These two forebody shapes apparently maintain aerodynamic symmetry by controlling the manner in which the vortices are shed after they originate at the forebody apex and by providing sufficient separation between the left and right vortices to prevent the vortex system on one side from becoming dominant. Apparently, the forebody vortex system that is created by such forebodies is stable when the left and right vortex systems are symmetrically displaced. For the other forebodies, the vortex system apparently becomes stable only when the vortex system is asymmetric. These results correlate with those of reference 7. It should be stressed in this discussion that the detailed fluid mechanics involved in the evolution and control of forebody vortex systems are not well understood. It is felt by some researchers that the key to controlling vortex shedding is to fix the separation line at which the vortex sheet sheds from the forebody. However, it is not clear whether this approach remains effective as one extends such separation devices aft of the immediate vicinity of the forebody apex. It should therefore be recognized that statements made in this paper referring to fixing separation lines are

only hypotheses that appear to explain the observed results. More detailed studies are needed to firmly substantiate the exact phenomena involved.

Effect of forebody add-on devices.- Previous tests (refs. 1, 2, 3, 5, 7, and 8) for other airplane configurations have indicated that forebody add-on devices such as nose strakes, nose booms, and trip wires can have large effects on aerodynamic symmetry at high angles of attack. Therefore, tests of such devices were conducted on selected forebodies to determine their effect on the lateral-directional asymmetry at zero sideslip. The data showing these effects are presented in figures 13 to 15.

Past investigations (e.g.,(ref. 2) have shown that small strakes placed near the tip of the nose of a pointed body can eliminate or minimize large asymmetric yawing moments at high angles of attack. A series of tests were therefore conducted to determine the effectiveness of strakes for the forebody having a circular cross section. The strakes tested were placed symmetrically in the XY-plane of the model, and the results are shown in figure 13. The effect of the strakes was to produce a well-defined point of separation near the nose apex. This effect resulted in a symmetrical flow field at all angles of attack and effective suppression of the asymmetries.

When the nose strake was applied to the 3.5 CIR forebody (fig. 13(a)), the large yawing-moment asymmetry was greatly reduced. Application of the same strake to the 3.5 EMAV forebody (fig. 13(b)) produced similar reductions in yawing moment, although less dramatic since the level of directional asymmetry for this forebody was considerably less than the asymmetry for the circular forebody.

The nose strakes were capable of producing as much as or more aerodynamic symmetry than was obtained with the shark or duckbill forebodies. (See fig. 13.) The flow mechanics involved would again appear to be those which fix the separation line for the nose vortex system. However, one should exercise caution before deciding, based only on aerodynamic symmetry, to use strakes in lieu of another forebody design. As shown in reference 5, application of nose strakes to the forebody can have quite detrimental effects on directional stability at high angles of attack; the result obtained is dependent upon the forebody cross section involved, as will be shown later in this report.

Data presented in figure 14 show that the addition of the nose boom (fig. 8) to the 3.5 CIR forebody produced a noticeable reduction in the magnitude of the yawing-moment asymmetry but did not eliminate it. Apparently, the shed vortex system was simply weakened as opposed to being radically changed by the nose boom. Figure 15 shows that when the helical trip wire was applied to the 3.5 CIR forebody, as shown in figure 9, the asymmetry in yawing moment was largely eliminated. This result would seem to indicate that the trip wire worked in a manner similar to the nose strake by fixing a separation line along the forebody which forced the shed vortex system to be symmetric. It is quite possible that further optimization of the trip wire size and location might provide further reductions in the yawing-moment asymmetry; however, the large effect seen in these data is sufficient to show that the helical pattern concept was quite effective.

Effect of other configuration features.- Additional tests were conducted to determine if interaction exists between the shed nose vortices and the other portions of the airframe as the vortices passed over the airframe. Previous tests of the model used in this investigation (ref. 11) indicated that deflection of the engine inlet cowls and the horizontal tails produced strong effects on the lateral-directional stability at high angles of attack. Another possible flow interaction could be caused by the vertical tails, which could extend into the trailing vortices. Therefore, additional model configuration variables were tested at $\beta = 0^{\circ}$ to assess the influence of the inlet cowl position, horizontal-tail deflection, and the vertical tail on the aerodynamic symmetry.

Figures 16 to 18 present results showing the influence of the aforementioned model configuration changes. Results presented in figure 16 show the effect of raising the inlet cowls to the undeflected cruise position. Although figure 16(a) indicates that this configuration change produced the onset of asymmetry for the 3.5 CIR forebody at a noticeably higher angle of attack, the magnitude of the asymmetry remained unchanged. Results shown in figure 16(b) for the 3.5 DKB forebody seem to show no significant influence of the inlet cowl deflection on the asymmetry. Figure 17 shows that the trailing-edge-up elevator deflection lowered the magnitude of the angle of attack required for the onset of asymmetry on the 3.5 CIR forebody, and the elevator deflection had no effect on the maximum level of asymmetry beyond onset. The data of figure 18 show that removal of the vertical tails had little or no effect on the yawing-moment asymmetries exhibited with the 3.5 CIR forebody.

Summary of aerodynamic lateral-directional symmetry results.- For the airframe configuration tested, large asymmetric yawing moments at $\beta = 0^{\circ}$ are only evident for the high-fineness-ratio forebodies. For the 3.5 fineness ratio (similar to the fineness ratio of the airplane of ref. 7), significant changes made to the basic airplane configuration, such as removal of the vertical tails, deflection of the inlet cowls, and deflection of the horizontal tails, seem to have only a secondary influence on the yawing-moment asymmetries observed. These results seem to confirm the conclusions drawn in previous forebody studies (refs. 1 to 5); that is, the asymmetric yawing moments are produced primarily by side forces which are developed on the fuselage forebody by the asymmetric vortex formation.

For the high-fineness-ratio forebodies, the forebody geometry was found to have a large influence on the measured yawing-moment asymmetries. The largest asymmetries were produced by the forebodies having smooth CIR or EMAH cross sections; the smallest asymmetry was produced by the EMAV forebody. The smallest yawing-moment asymmetries were obtained on forebodies where the separation line for the shed vortices was fixed, at least at the forebody apex, to produce symmetric shedding. These results were obtained with nose strakes, the SHK and DKB forebodies, and the trip wire. However, as will be discussed in the next section, selection of the desired forebody shape should be based not only on minimizing asymmetries, but also on effects of the forebody on directional and lateral stability at high angles of attack.

Lateral-Directional Stability

Additional testing was conducted to evaluate the influence of forebody geometry on the lateral-directional stability characteristics of the subject configuration. As in the previous section, the results are presented to show the effects of fineness ratio; cross-sectional shape; nose strakes, trip wires, and booms; and model configuration changes.

Effect of forebody fineness ratio.- The effect of forebody fineness ratio on lateral-directional stability is shown in figure 19 for the 2.3 CIR, 3.5 CIR, 2.3 EMAH, and 3.5 EMAH forebodies. In figure 19(a), the data show that directional instability occurred above 22° α for both the 2.3 CIR and 3.5 CIR forebodies. Above 25° α (as might be expected), the longer forebody (3.5 fineness ratio) produced the highest levels of directional instability, whereas the configuration with forebody removed (blunt nose) shows the lowest level of directional instability. It is also interesting to note that the 3.5 CIR forebody experienced a noticeable loss in positive effective dihedral C_{l_β} between 20° and 40° α. Therefore, extending the CIR forebody degraded both directional and lateral stability at high angles of attack.

In contrast to the foregoing results, the data presented for the EMAH forebody in figure 19(b) shows increased directional stability above 30° α for the 3.5 fineness ratio. These results show that the same beneficial forebody effects found for the aircraft configuration tested in reference 5 could also be obtained on the aircraft configuration used in this study. This observation tends to further substantiate the conclusion that proper forebody design can produce generally favorable contributions to directional stability at high angles of attack. Comparison of the onset and level of directional instability between the blunt nose and the 2.3 EMAH forebody shows that the 2.3 EMAH forebody produces a very small improvement in directional stability as compared with the 3.5 EMAH forebody. This observation indicates that fineness ratio has a strong influence on the directional stability for this cross-sectional shape. Unfortunately, both the 2.3 and 3.5 EMAH forebodies produce a large loss in effective dihedral between 25° and 40° α. Additional data from further static-force and flow-visualization tests would be needed to define the phenomenon involved in this loss of dihedral; it can only be hypothesized that the interaction of the vortices shed from the forebody over the leeward wing at nonzero sideslip probably causes the flow to remain attached over that wing and thereby produces destabilizing rolling moments.

Effect of cross-sectional shape.- Since the results presented in the previous section showed the greatest influence of forebody cross-sectional shape to exist at the higher fineness ratio, the influence of cross-sectional shape is examined in this section for the highest fineness ratio tested. The effect of forebody cross section on lateral-directional stability is shown in figure 20. The data show that the level of directional stability for the forebodies tested varies over a large range above 10° to 15° α and is strongly dependent on the forebody cross section. At the high fineness ratio, the CIR and EMAV cross-sectional shapes degraded directional stability, but the EMAH, SHK, and DKB cross-sectional shapes improved directional stability. The data also show a loss in effective dihedral for the CIR, EMAH, and SHK forebodies

between 20° and 40° α. It is particularly interesting to note that the DKB forebody is the only one of the three forebodies producing stable values of both C_{n_β} and C_{l_β} in this angle-of-attack range. Such a configuration would be expected to exhibit good dynamic stability in the stall. As will be noted later, a similar effect was obtained by use of nose strakes.

Presented in figure 21 are data showing the effect of the vertical tails on the model configuration with the CIR, SHK, and DKB 3.5 fineness-ratio forebodies. For all these forebodies, the vertical tails are directionally stabilizing up to about 25° α; above 25° α, the vertical tails are somewhat directionally destabilizing. It is particularly interesting that above 25° α, the directional stability observed in the complete configuration for the SHK and DKB forebodies was produced by the forebody and not by the vertical tails. This result again correlates well with results of references 6 and 7. It is also evident that above 20° α the vertical tails produce only a small effect on C_{l_β} for the three forebodies shown. Therefore, one may conclude that the loss in C_{l_β} produced by the SHK forebody is not due to any adverse influence of the vertical tails but is more likely a strong interaction between the nose vortices and the wing, as hypothesized earlier.

Effect of forebody add-on devices.- It has been shown earlier that several forebody modifications, including nose strakes, nose trip wires, and nose booms, can significantly influence forebody aerodynamics at high angles of attack. Further tests were made to determine the influence of such devices on lateral-directional stability at high angles of attack; the results are presented in figures 22 to 24.

Figure 22 presents lateral-directional data showing the influence of the nose strakes on the 3.5 CIR, 3.5 EMAV, and 2.3 CIR forebodies. Figures 22(a), (b), and (c) show that the nose strakes essentially eliminated the unstable values of C_{n_β} above 20° α for all three forebodies. The vertical-tail-off data presented in figure 22(d) for the 3.5 CIR forebody with nose strakes indicate that the effect of the nose strakes on C_{n_β} is quite similar to that seen in figure 21 for the 3.5 EMAH, SHK, and DKB forebodies in that the configuration is directionally stable at high angles of attack with or without the vertical tails. However, in contrast to the effect of the 3.5 EMAH and SHK forebodies, the effect of the nose strakes on C_{l_β} is quite stabilizing at high angles of attack, as was the DKB forebody.

It was shown earlier that placing the helical trip wire on the 3.5 CIR forebody greatly reduced the yawing-moment asymmetries. Figure 23 presents data showing the influence of the trip wire on lateral-directional stability. There is little effect on C_{n_β} below 30° α and some modest favorable influence at higher angles of attack; the influence on C_{l_β} is minimal. These

results, therefore, indicate that such a device as the helical trip wire has its largest effect in forcing symmetric separation of the nose vortex system at $\beta = 0^{\circ}$, thereby avoiding the development of large side forces on the nose at high angles of attack. There appear to be no significant effects of the trip wire on stability.

In an effort to assess the sensitivity of the model aerodynamics to geometric changes that may occur on a test or production airplane, several configurations were tested to measure the influence of nose boom installations. Results obtained for the CIR and DKB forebodies are presented in figure 24. Results in figure 24(a) for the 3.5 CIR forebody show little or no influence of the nose boom below 40° α. At higher angles of attack, it appears the nose boom degrades static directional stability. In contrast to the results for the 3.5 CIR forebody, results presented in figure 24(b) for the 3.5 DKB forebody show that the nose boom installation noticeably degraded both C_{n_β} and C_{l_β} above 25° α, and resulted in unstable values of C_{n_β} between 25° and 30° α. Despite the degrading effect of the nose boom, the stabilizing influence of the DKB forebody on C_{n_β} is still evident. These results, however, do show that the aerodynamics of this particular forebody can be quite sensitive to what might usually be considered "minor" changes made to the nose. In attempting to conduct flight evaluations of possible stability improvements to be obtained from novel forebody designs, it is clear that one should be quite cautious when making changes to the forebody geometry to accommodate test equipment or air-data sensors. The stability degradation produced by the nose boom installation in the subject tests represents a very significant loss in stability for the DKB forebody.

Effect of other configuration features.- Results presented in figure 25 show that the effect of raising the inlet cowls to the undeflected position was dependent upon the particular forebody design used. The influence of cowl position on directional stability was much more pronounced for the 3.5 CIR forebody (fig. 25(a)) than for the DKB forebody (fig. 25(b)). On the other hand, the cowl deflection influence on lateral stability is similar for the two forebodies. The primary difference in the cowl effect on lateral stability between the two forebodies was that raising the inlet cowl produced a larger loss of dihedral effect for the DKB forebody. The point to be made from these results is that there seems to be an interaction of the forebody flow field and the wing-body flow field. This interaction is sufficiently strong to change the influence of a configuration variable, such as inlet cowl position, when a significant change in forebody design is made.

The influence of horizontal-tail deflection is presented in figure 26 for the 3.5 CIR and DKB forebodies. For both forebody configurations, deflection of the horizontal tail (in an airplane nose-up sense) produces a reduction in both directional and lateral stability at a given angle of attack. The loss in both C_{n_β} and C_{l_β} above 20° α due to tail deflection appears to be slightly more severe for the DKB forebody. This result for the effect of horizontal-tail deflection, together with similar results for the inlet cowl deflection, indicates that the C_{l_β} of the total configuration with the DKB

forebody is considerably more sensitive to other configuration variables than is the C_{l_β} associated with the more conventional 3.5 CIR forebody. The primary conclusion from this brief evaluation of effects of other configuration features is as noted before: changes to forebody design may significantly change the influence which other configuration features have on the stability characteristics of the configuration.

Longitudinal Characteristics

Results presented in this paper, as well as already published results (refs. 2 to 5), indicate that very strong vortex flows can develop on long, slender forebodies at high angles of attack. Moreover, the rolling-moment data already discussed in this report indicate a possible significant interaction of the nose vortex system with the wing-body flow field. Therefore, one might suspect noticeable effects of the nose vortex system on lift and pitching-moment characteristics. For example, reference 12 presents in-depth results concerning the effects of nose strakes on longitudinal and directional stability at high subsonic speeds and investigates the influence of strake sizing. Although the emphasis in this paper has been to assess the favorable effects which might be obtained on lateral-directional aerodynamics as a result of forebody design, it is also quite important to evaluate what impact such novel forebody designs may have on longitudinal characteristics at high angles of attack. Therefore, longitudinal aerodynamics were measured for most of the forebody designs tested over the aforementioned ranges of angles of attack and sideslip. Selected results of some tests are presented in figures 27 to 31 for zero and nonzero sideslip conditions.

Effect of forebody on stability at $\beta = 0^\circ$.- Figures 27 and 28 show the influence of forebody design on the variation with angles of attack of lift, drag, and pitching-moment coefficients at $\beta = 0^\circ$. Figure 27 shows the influence of forebody fineness ratio for the CIR and EMAH forebodies. As either forebody length is increased, there is an apparent forward shift in the center of lift which produces a noticeable reduction in longitudinal stability C_{m_α} near and above maximum lift. In the two cases shown, the total values of C_{m_α} actually become neutral to unstable. However, these results are all presented for a fixed center of gravity and such forebody extensions might very well involve a forward movement of the airplane center of gravity.

Presented in figure 28 is a summary of the longitudinal characteristics measured for the longer forebody designs of various cross-sectional shapes with a 3.5 fineness ratio. As one might expect, these results show that the EMAV forebody produces the fewest adverse effects on stability since it projects the least planform area. Further, the results indicate that all of the other forebody cross sections tested produce varying degrees of pitch instability, with the SHK design producing the largest loss of pitch stability near maximum lift. It is evident from these results that extensions of the forebody of this airplane configuration can produce reductions in longitudinal stability which are quite dependent on the forebody cross-sectional shape, as well as on

the increased planform area produced by the extension. Apparently, the cross-sectional shape greatly influences the character of the vortices formed on the nose; these nose vortices, in turn, determine the aerodynamic lift generated by the particular forebody.

Effect of sideslip.- Additional longitudinal tests were made over a range of sideslip at specific angles of attack to determine the influence of forebody geometry on pitching moment. Maneuvers at high angles of attack often generate significant sideslip and require reasonably tight control of angle of attack to prevent excursions in angle of attack, which may result in loss of control. It is, therefore, important to determine if there is any strong dependence of pitching moment on sideslip which might produce uncommanded excursions in angle of attack during high angle-of-attack maneuvering.

The results of the investigation of sideslip effects are presented in figures 29 to 31 which show the variation of C_m with β for various angles of attack. The influence of fineness ratio on the EMAH forebody is presented in figure 29. For the two higher angles of attack (30^o and 40^o), there is a noticeable loss in restoring pitching moment with increasing β when the forebody length is increased. Beyond 5^o β, a mild pitch instability ($C_{m_\alpha} > 0$) is evident for the higher fineness ratio. Figure 30 presents the results for the influence of the EMAV and DKB forebody cross-sectional shapes. The DKB configuration clearly experiences a very substantial loss of restoring pitching moment at sideslip in contrast to the EMAV forebody which appears relatively insensitive to β. A maneuver producing 10^o to 15^o β with the DKB forebody could be expected to result in a 50-percent loss of restoring pitching moment, roughly half the pitching moment available from a full nose-up deflection of the horizontal tail on this model. The effects of various forebody add-on devices (nose strakes and helical trip wire) on the 3.5 CIR forebody at 32.5^o α are presented in figure 31. The nose strake is the only modification producing a noticeable influence (adverse) on the sideslip dependence of C_m. It is interesting to recall at this point that the nose strake was also much more effective in influencing (favorably) lateral-directional stability than was the trip wire. The trip wire also provided good suppression of yawing-moment asymmetries without producing any adverse effects on longitudinal characteristics.

The foregoing results seem to indicate that changes to forebody designs which produce strong, stable nose-vortex systems capable of strongly influencing lateral-directional stability near maximum lift are also capable of producing substantial losses in restoring pitching moment at sideslip. Such effects of forebody geometry on longitudinal aerodynamic stability should therefore certainly be investigated as part of any effort directed at developing forebody designs similar to those investigated in this study. Although the effects of C_m shown in this study may not raise great concern for an airframe which is inherently stable in pitch, they could be a significant cause for concern in a configuration balanced to use relaxed static stability. For such a configuration, the total airplane stability at high angles of attack is provided by a static stability augmentation system driving the horizontal tail. In this situation, significant unexpected nose-up pitching moments occurring at sideslip may be sufficiently large to saturate the longitudinal stability augmentation system and result in uncontrollable excursions in angle of attack.

CONCLUDING REMARKS

A low-speed wind-tunnel investigation has been conducted using a 0.10-scale model of a modern fighter configuration to study the influence of fuselage forebody design on high-angle-of-attack aerodynamics. The various forebody designs tested can have a large influence on the high-angle-of-attack aerodynamic stability of the airplane configuration. Specific results are best summarized in three areas: aerodynamic symmetry, lateral-directional stability, and longitudinal stability.

At high angles of attack, it is desirable for an airplane configuration to have small, near-zero values of rolling and yawing moments at zero sideslip; the presence of large asymmetric moments at high angles of attack is undesirable in that they can contribute to loss of control and possible spin entry. Results of the present tests indicate that significant aerodynamic asymmetries were evident only for the higher fineness ratio forebodies tested. At the high fineness ratio (3.5), the asymmetries were strongly influenced by forebody cross-sectional shape and special add-on devices. The largest asymmetries (primarily yawing moment) were exhibited by the forebodies having circular CIR or elliptical (major axis horizontal) EMAH cross-sectional shapes (shapes typical of current fighter forebodies); these asymmetries could be largely eliminated on these forebodies by proper application of nose strakes or a trip wire applied in a helical pattern. Minimal asymmetries were observed on the other forebodies tested. Installation of a typical flight test nose boom was found to reduce the asymmetries but not eliminate them. Such configuration variables as the engine inlet cowl deflection, horizontal-tail deflection, and vertical tails were found to have small effects on aerodynamic symmetry.

Results indicated that the forebody design features of fineness ratio, cross-sectional shape, and add-on devices (e.g., strakes) can strongly influence both lateral and directional stability at high angles of attack - both favorable and adverse effects were measured. The influence of cross-sectional shape and add-on devices was consistently evident at both low and high fineness ratios but was largest at the higher fineness ratio.

At the high fineness ratio, circular CIR and major-axis-vertical elliptical EMAV cross-sectional shapes degraded directional stability, but the major-axis-horizontal elliptical EMAH, shark SHK, and duckbill DKB cross-sectional shapes improved directional stability. Addition of nose strakes to the CIR and EMAV forebodies provided improved directional stability. Lateral stability was degraded by the CIR, EMAH, and SHK forebodies, but lateral stability was improved by the other forebodies and by add-on devices. Application of the helical trip wire to the circular forebody had little effect on stability, but use of the nose boom on several forebodies produced an adverse effect on directional stability. Finally, the forebody design for the particular airplane configuration tested was found to significantly influence the effect on stability of such configuration variables as engine inlet cowl deflection and horizontal-tail deflection; such influence was not observed on the effect of the vertical tails.

Most of the changes made to the high-fineness-ratio forebodies to provide improved directional stability and symmetry, such as changes to cross-sectional

shape or addition of nose strakes, produced noticeable reductions in longitudinal stability near maximum lift. Similar significant reductions in longitudinal stability occurred due to sideslip for most of the forebody treatments which, however, had improved directional stability. An outstanding exception to this trend of degrading pitch stability was the helical trip wire; it produced aerodynamic symmetry without adversely affecting pitch stability.

Results of this investigation, when combined with forebody test results obtained in other studies, indicate that substantial tailoring of stability at high angles of attack can be accomplished through proper forebody design. However, these results also show that the total effect of the forebody on stability (including longitudinal, lateral, and directional) must be examined carefully for each airplane since a particular forebody change can produce both favorable and adverse effects on stability and can strongly influence the effects of other configuration variables. Moreover, results of other investigations have shown that forebody design can strongly influence aerodynamic damping derivatives in the stall and airplane developed spin characteristics; therefore, such additional effects should be considered in the selection of a particular forebody design.

Langley Research Center
National Aeronautics and Space Administration
Hampton, VA 23665
November 20, 1979

REFERENCES

1. Spearman, M. Leroy: Some Factors Affecting the Static Longitudinal and Directional Stability Characteristics of Supersonic Aircraft Configurations. NACA RM L57E24a, 1957.

2. Chambers, Joseph R.; Anglin, Ernie L.; and Bowman, James S., Jr.: Effects of a Pointed Nose on Spin Characteristics of a Fighter Airplane Model Including Correlation With Theoretical Calculations. NASA TN D-5921, 1970.

3. Coe, Paul L., Jr.; Chambers, Joseph R.; and Letko, William: Asymmetric Lateral-Directional Characteristics of Pointed Bodies of Revolution at High Angles of Attack. NASA TN D-7095, 1972.

4. Keener, Earl R.; and Chapman, Gary T.: Onset of Aerodynamic Side Forces at Zero Sideslip on Symmetric Forebodies at High Angles of Attack. AIAA Paper No. 74-770, Aug. 1974.

5. Grafton, Sue B.; Chambers, Joseph R.; and Coe, Paul L., Jr.: Wind-Tunnel Free-Flight Investigation of a Model of a Spin-Resistant Fighter Configuration. NASA TN D-7716, 1974.

6. McLemore, H. Clyde; and Parlett, Lysle P.: Low-Speed Wind-Tunnel Tests of a 1/10-Scale Model of a Blended-Arrow Supersonic Cruise Aircraft. NASA TN D-8410, 1977.

7. Edwards, O. R.: Northrop F-5F Shark Nose Development. NASA CR-158936, 1978.

8. Rao, Dhanvada M.: Side-Force Alleviation on Slender, Pointed Forebodies at High Angles of Attack. AIAA Paper 78-1339, Aug. 1978.

9. Lorincz, Dale J.: A Water Tunnel Flow Visualization Study of the F-15. NASA CR-144878, 1978.

10. Standard for Metric Practice. E 380-76, American Soc. Testing & Mater., 1976.

11. Gilbert, William P.: Free-Flight Investigation of Lateral-Directional Characteristics of a 0.10-Scale Model of the F-15 Airplane at High Angles of Attack - COORD. No. AF-AM-010. NASA TM SX-2807, U.S. Air Force, 1973.

12. Polhamus, Edward C., and Spreemann, Kenneth P.: Effect at High Subsonic Speeds of Fuselage Forebody Strakes on the Static Stability and Vertical-Tail-Load Characteristics of a Complete Model Having a Delta Wing. NACA RM L57K15a, 1958.

TABLE I.- DIMENSIONAL CHARACTERISTICS OF THE MODEL

Overall fuselage length (forebody fineness ratio = 2.3), m (ft)	1.905 (6.25)
Overall fuselage length (forebody fineness ratio = 3.5), m (ft)	2.076 (6.81)
Forebody base diameter	0.141 (0.461)
Wing:	
Span, m (ft)	1.305 (4.281)
Area, m^2 (ft^2)	0.565 (6.08)
Mean aerodynamic chord, m (ft)	0.485 (1.59)
Leading edge of $\bar{c}$ rearward of root-chord leading edge, m (ft)	0.261 (0.857)
Aspect ratio	3.01
Taper ratio	0.25
Sweepback of leading edge, deg	45
Dihedral, deg	-1
Incidence, deg	0
Horizontal tails:	
Area (each), m^2 (ft^2)	0.0557 (0.60)
Span, m (ft)	0.253 (0.829)
Aspect ratio	2.05
Taper ratio	0.34
Sweepback of leading edge, deg	50
Dihedral, deg	0
Hinge-line location, percent root chord	60.9
Vertical tails:	
Area (each), m^2 (ft^2)	0.0582 (0.626)
Span, m (ft)	0.315 (1.032)
Taper ratio	0.266
Sweepback of leading edge, deg	36.57

TABLE II.- SUMMARY OF LATERAL-DIRECTIONAL RESULTS

[Changes produced by each different forebody are compared with the basic model forebody, the 2.3 CIR forebody. Changes produced by add-on devices are compared with the characteristics of the forebody to which the device was added]

Forebody	Add-on device	Effects (a)		
		C_{n_β}	C_{l_β}	Aerodynamic symmetry
2.3 CIR	None	----	----	----
	Strakes	PRO	PRO	N.E.
3.5 CIR	None	ADV	ADV	ADV
	Strakes	PRO	PRO	PRO
	Nose boom	ADV	N.E.	PRO
	Trip wire	N.E.	N.E.	PRO
2.3 EMAH	None	PRO	ADV	N.E.
3.5 EMAH	None	PRO	ADV	ADV
3.5 EMAV	None	ADV	N.E.	ADV
	Strakes	PRO	PRO	PRO
3.5 DKB	None	PRO	PRO	N.E.
	Nose boom	ADV	ADV	*
3.5 SHK	None	PRO	ADV	N.E.

[a]Individual effects indicated are relative and are designated as follows:

ADV	adverse; degrades configuration
PRO	favorable; improves configuration
N.E.	little or no effect
*	not measured

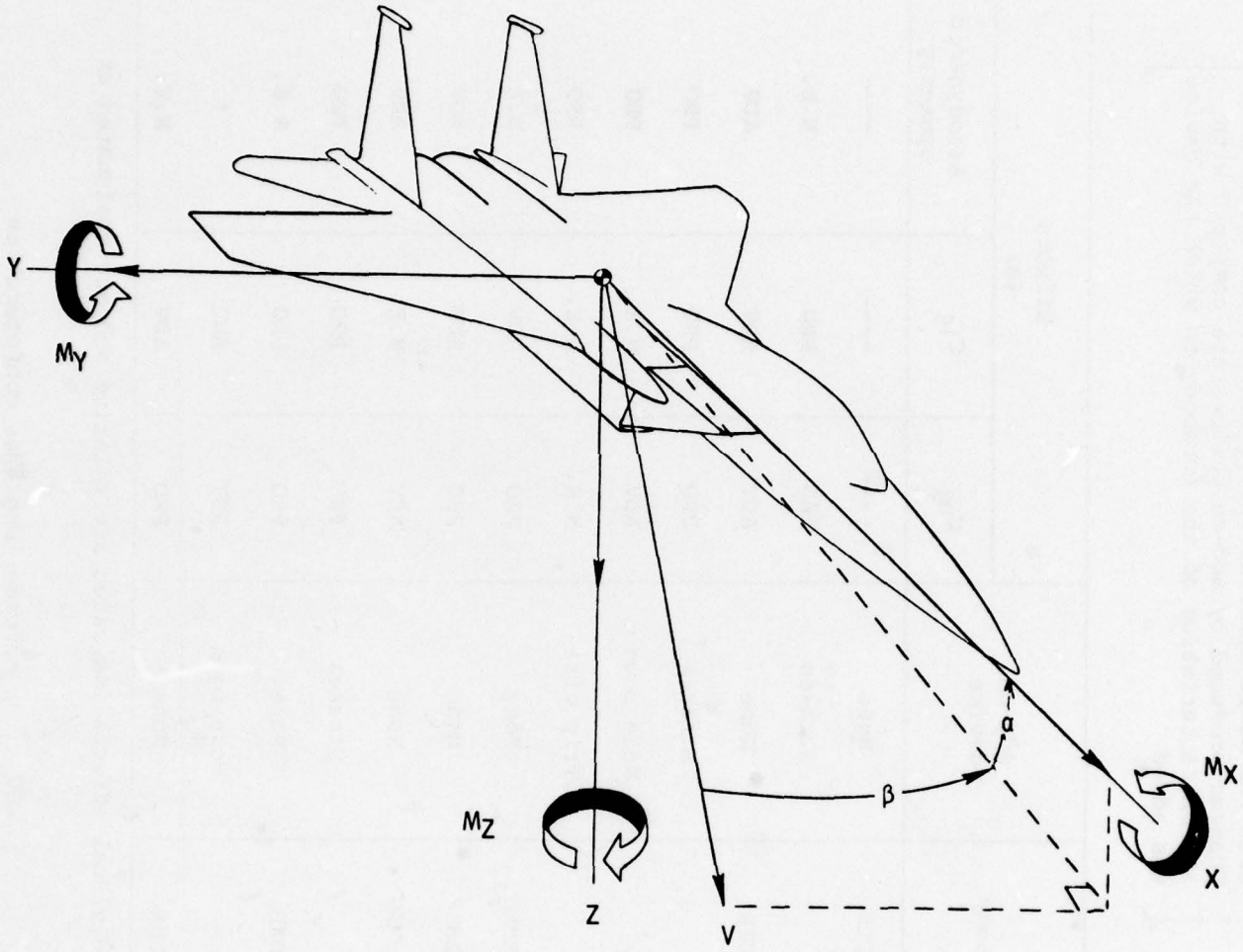

Figure 1.- Body axes reference system.

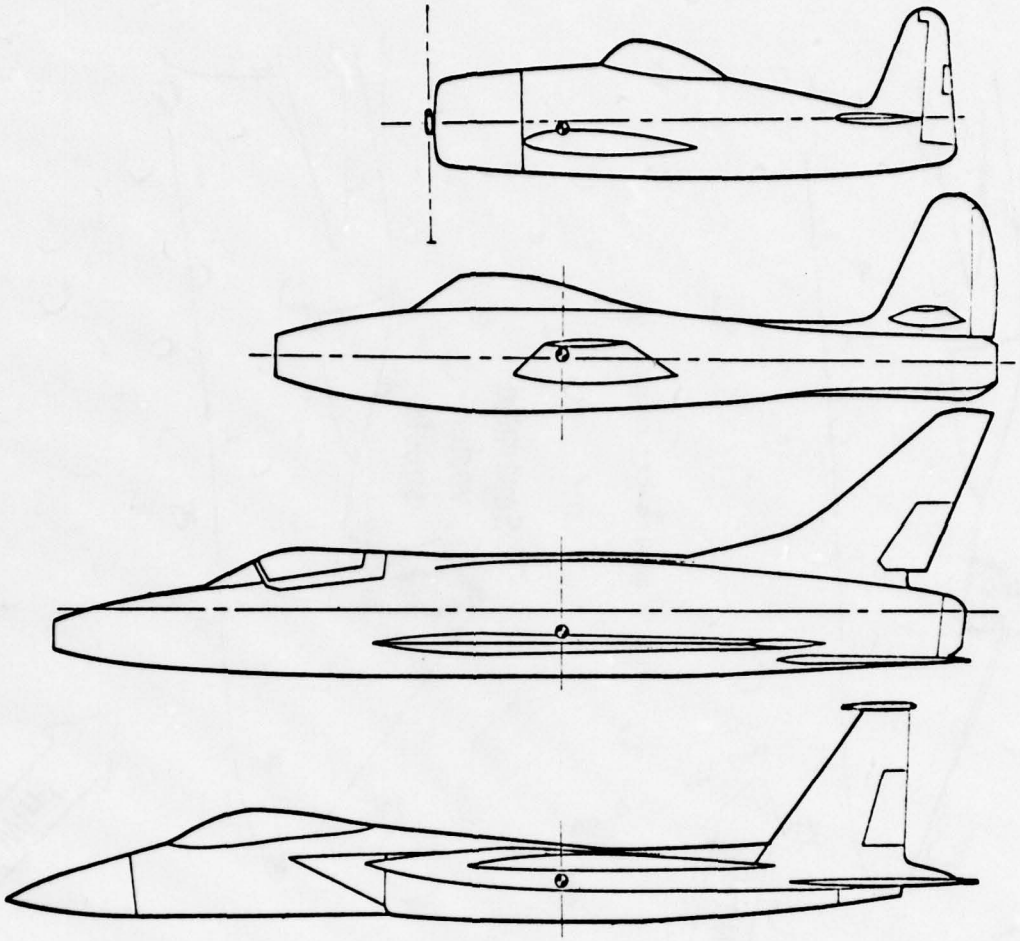

Figure 2.- Variations in fighter airframe geometry.

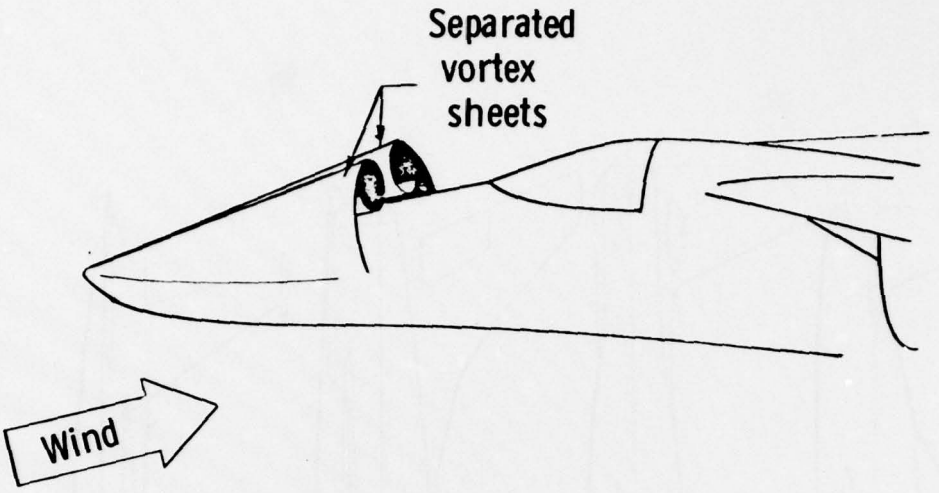

(a) Low angles of attack.

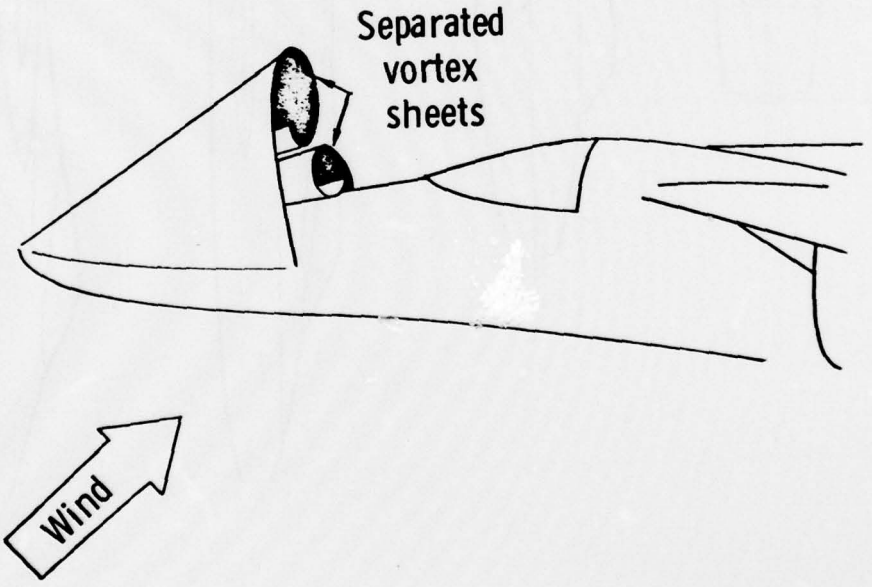

(b) High angles of attack.

Figure 3.- Sketches of separated vortex sheets on fuselage forebody.

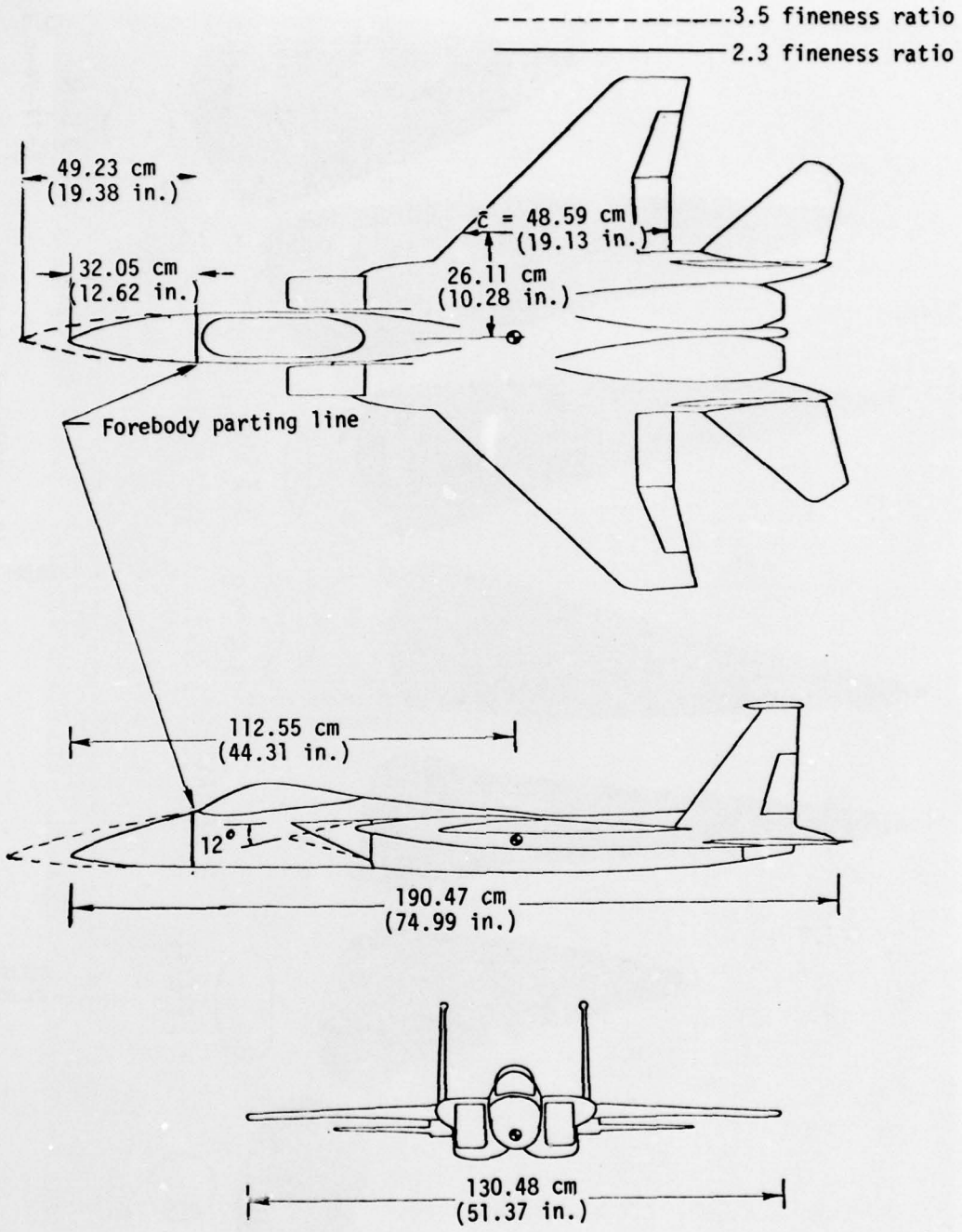

Figure 4.- Three-view sketch of model with 2.3 and 3.5 fineness ratio forebodies.

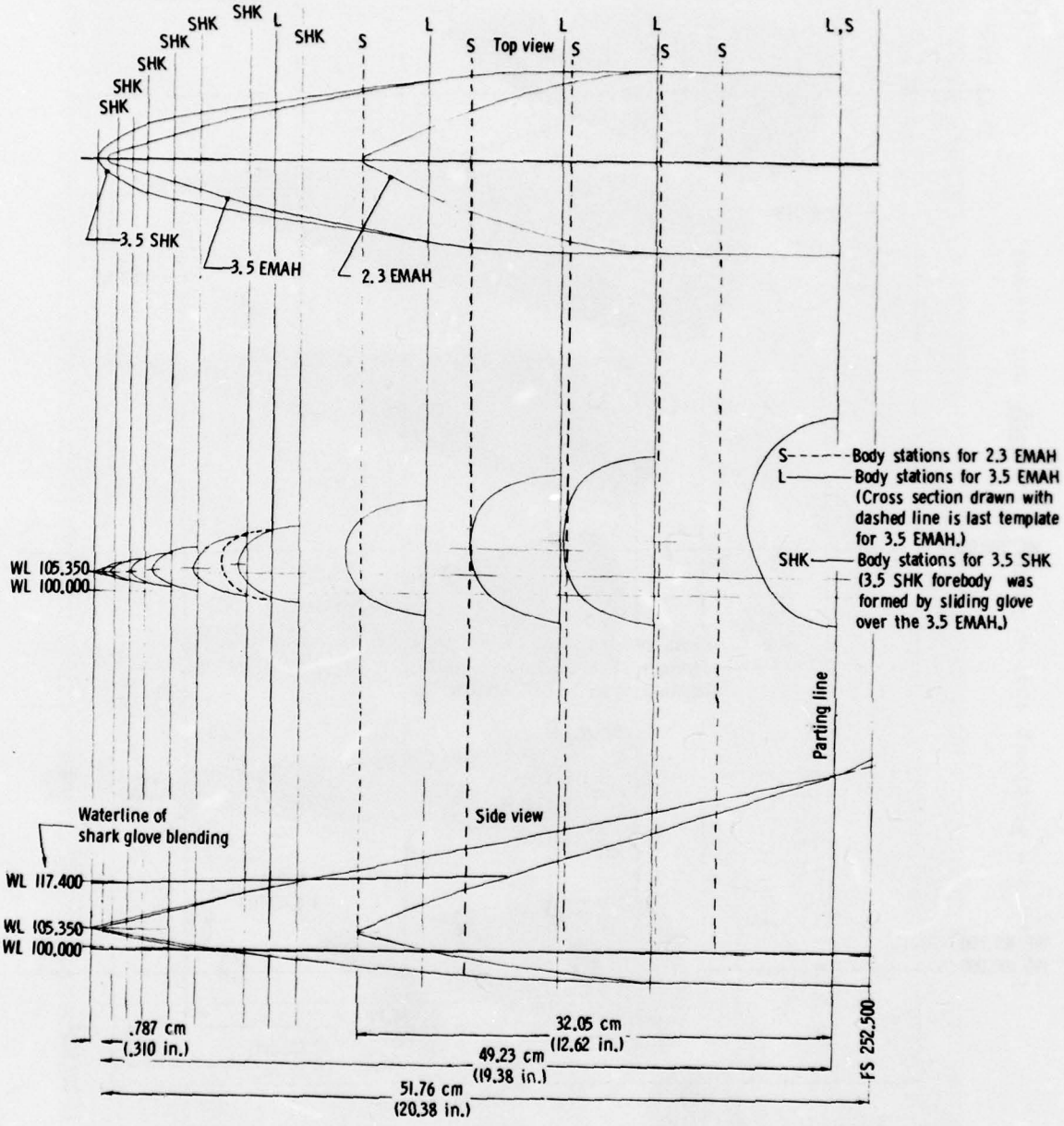

(b) Composite drawings of the 3.5 EMAH, 2.3 EMAH, and 3.5 SHK forebodies.

Figure 6.- Continued.

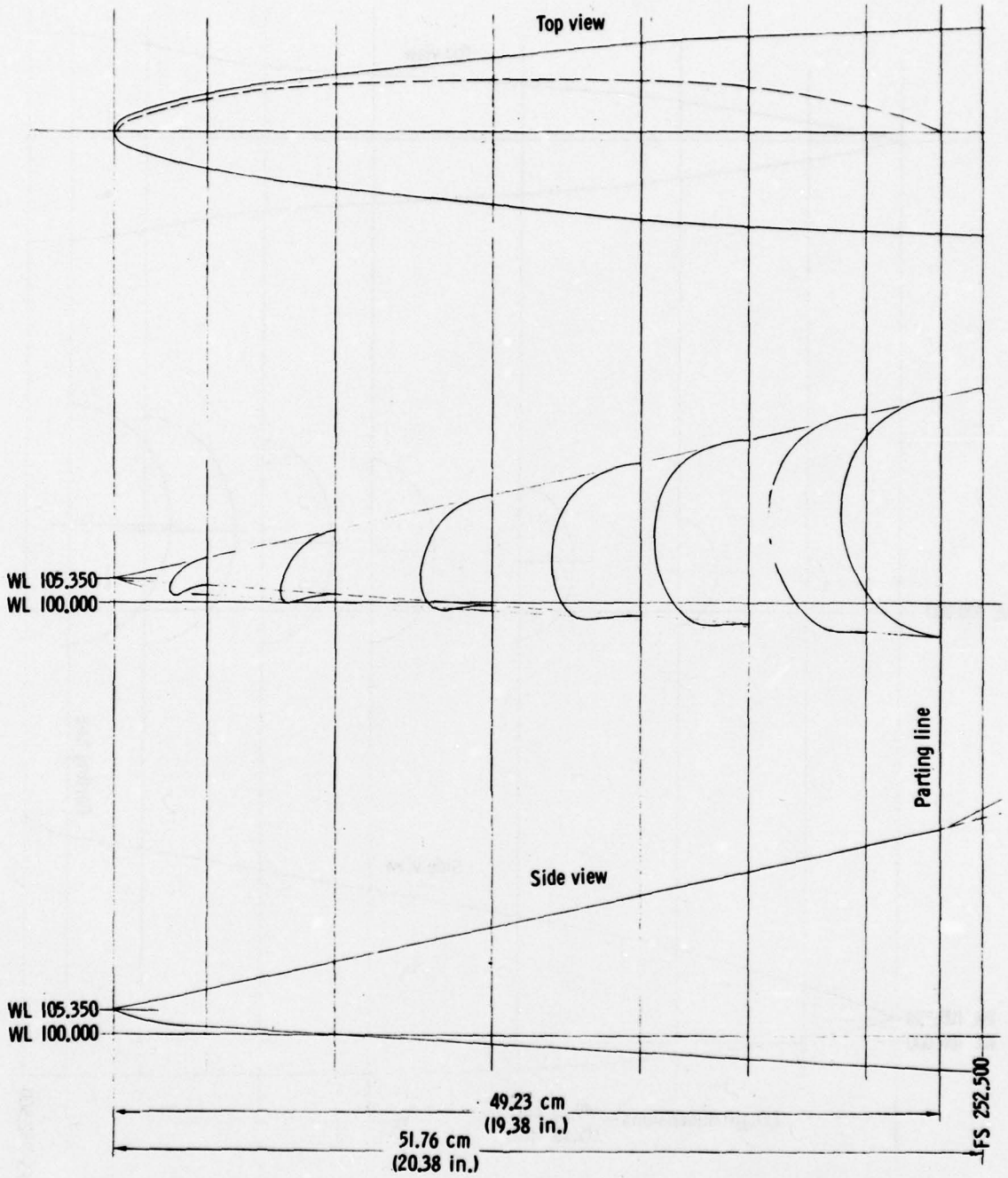

(c) Drawing of 3.5 DKB forebody.

Figure 6.- Continued.

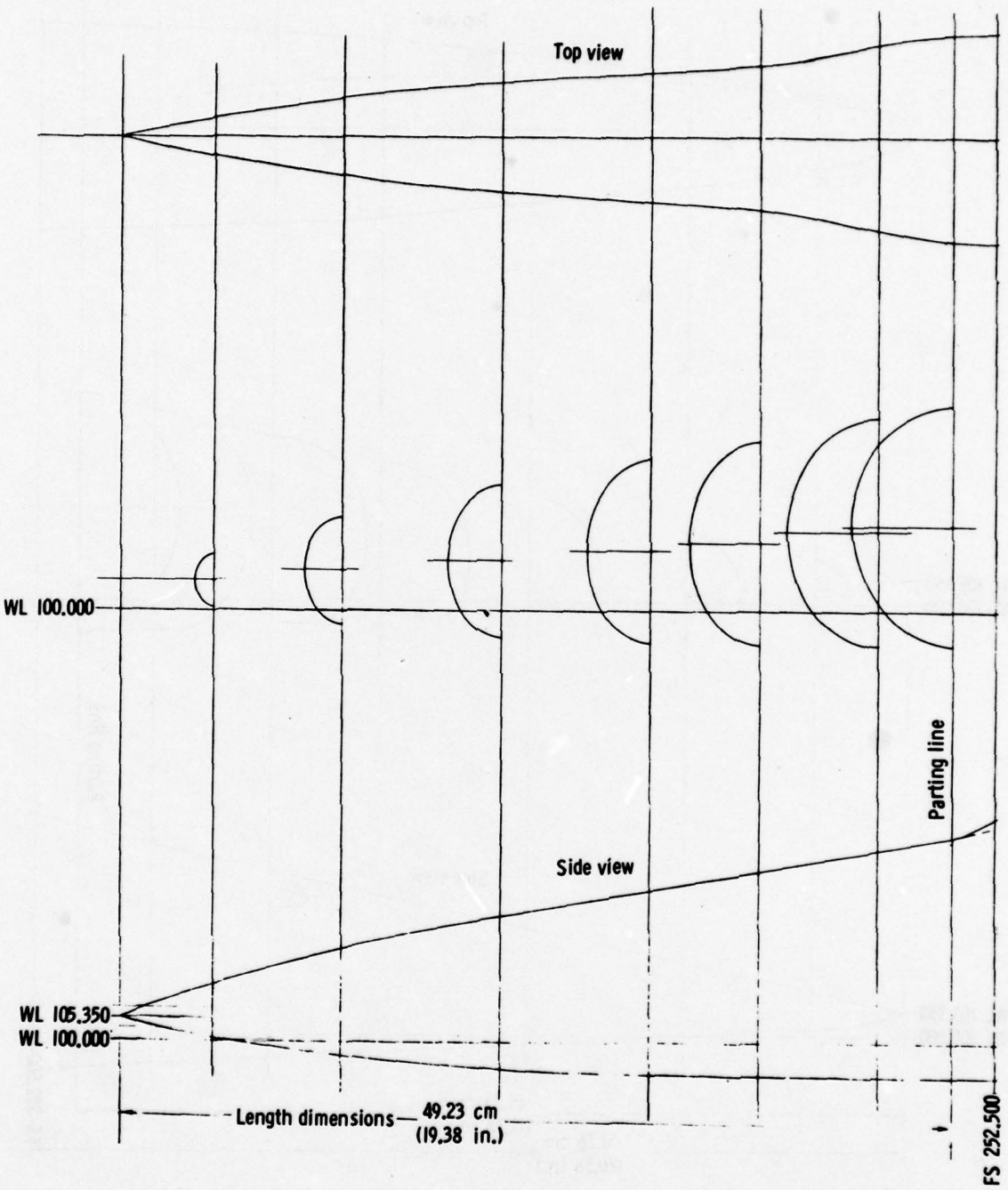

(d) Drawing of 3.5 EMAV forebody.

Figure 6.- Concluded.

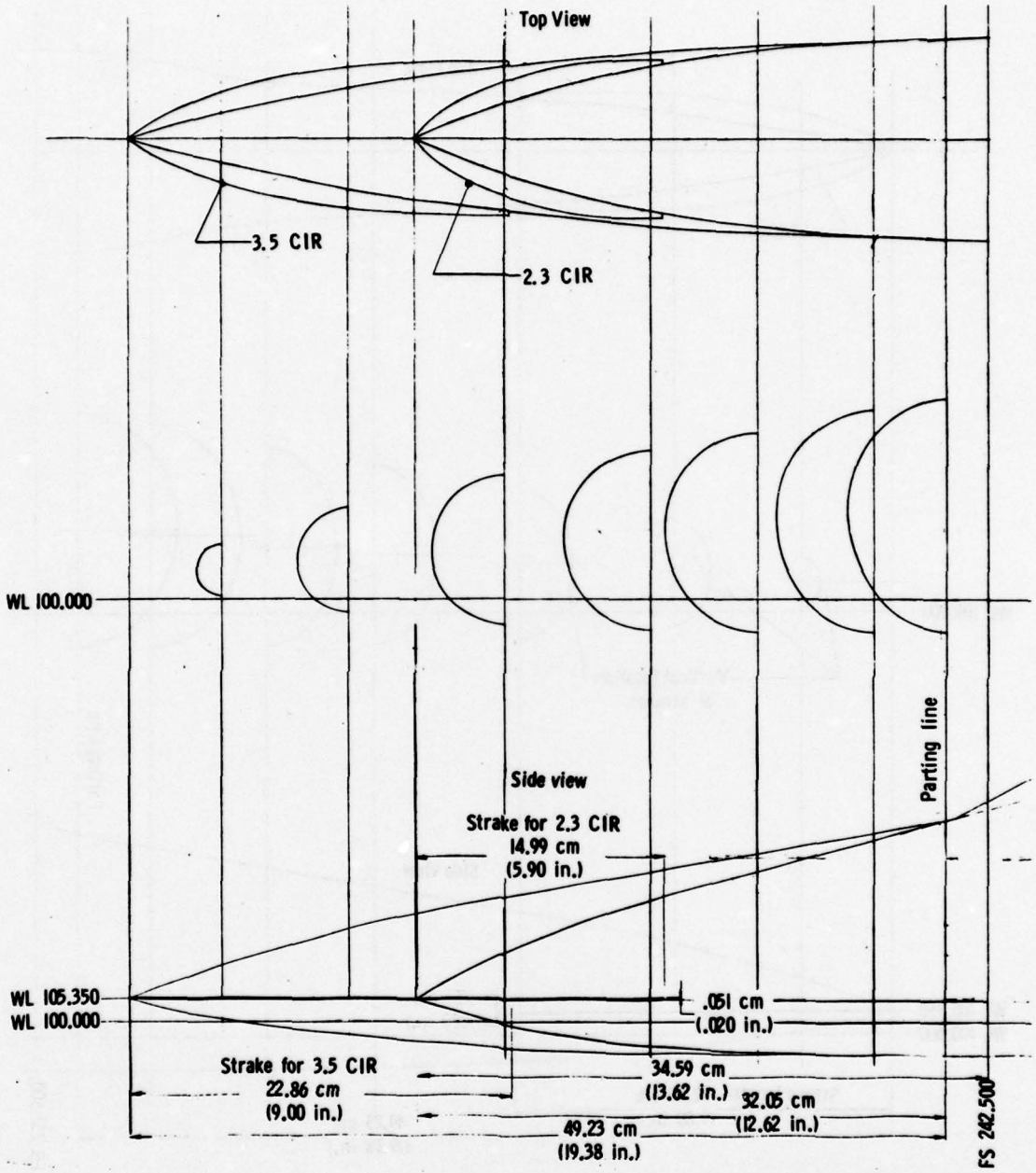

(a) Strake design and location as applied to 2.3 CIR and 3.5 CIR forebodies.

Figure 7.- Sketches of strake arrangements used on forebodies.

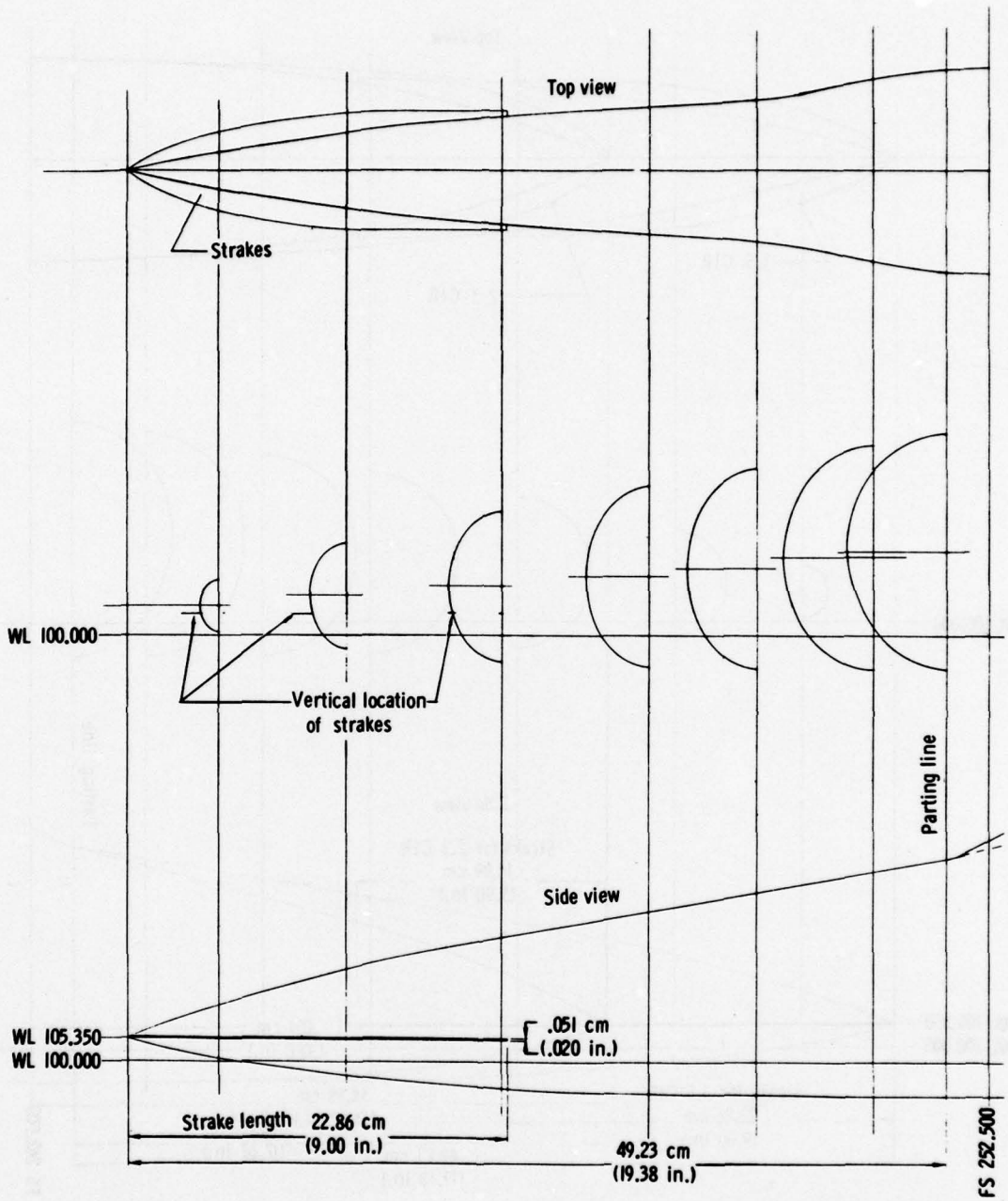

(b) Strake design and location used on 3.5 EMAV forebody.

Figure 7.- Concluded.

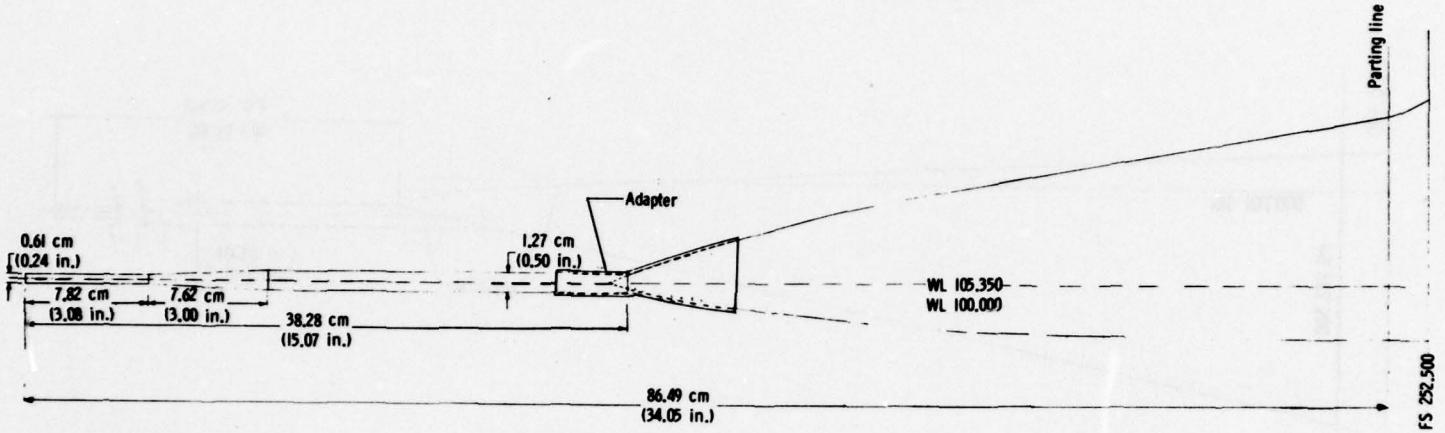

(a) Nose boom mounting used on 3.5 CIR forebody.

Figure 8.- Description of nose boom configurations.

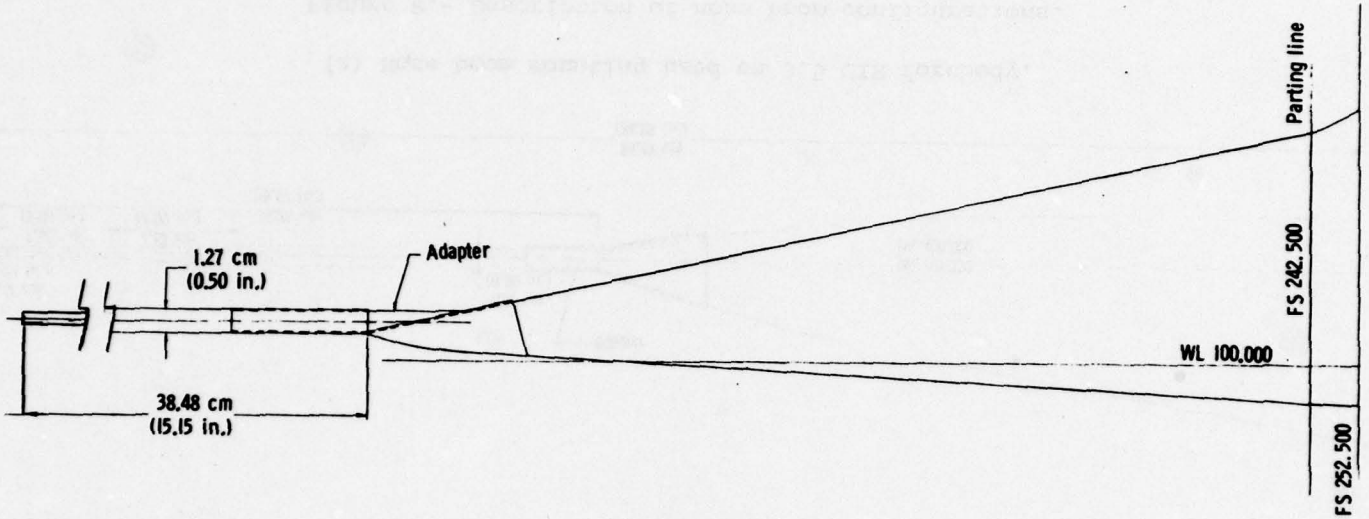

(b) Nose boom mounting used on 3.5 DKB forebody.

Figure 8.- Concluded.

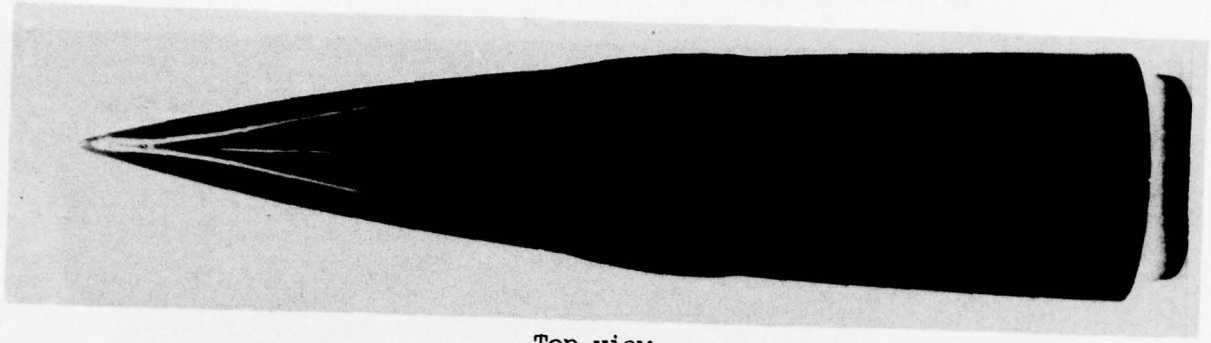

Top view

L-78-2062.1

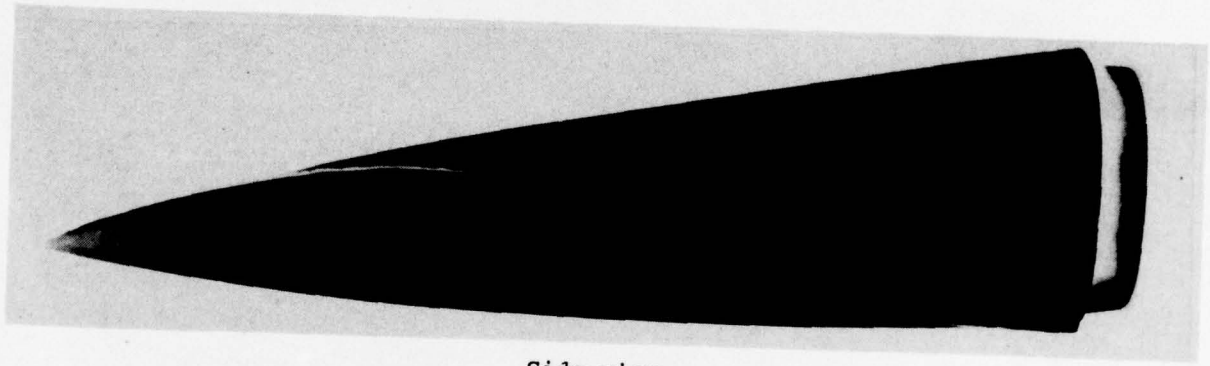

Side view

L-78-2059.1

Figure 9.- Photograph of trip-wire installation on 3.5 CIR forebody.

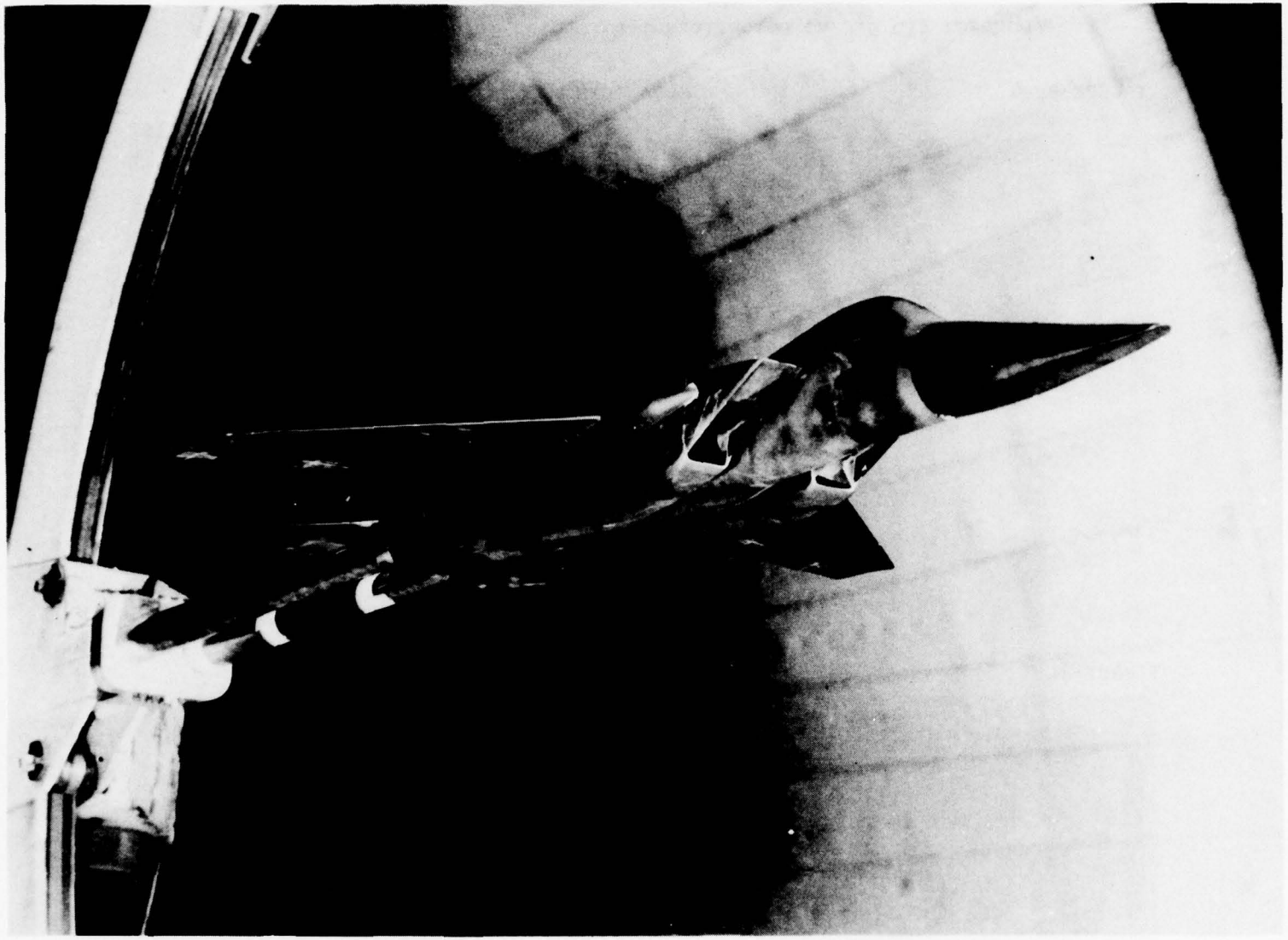

L-78-791

Figure 10.- Photograph of model with 3.5 DKB forebody.

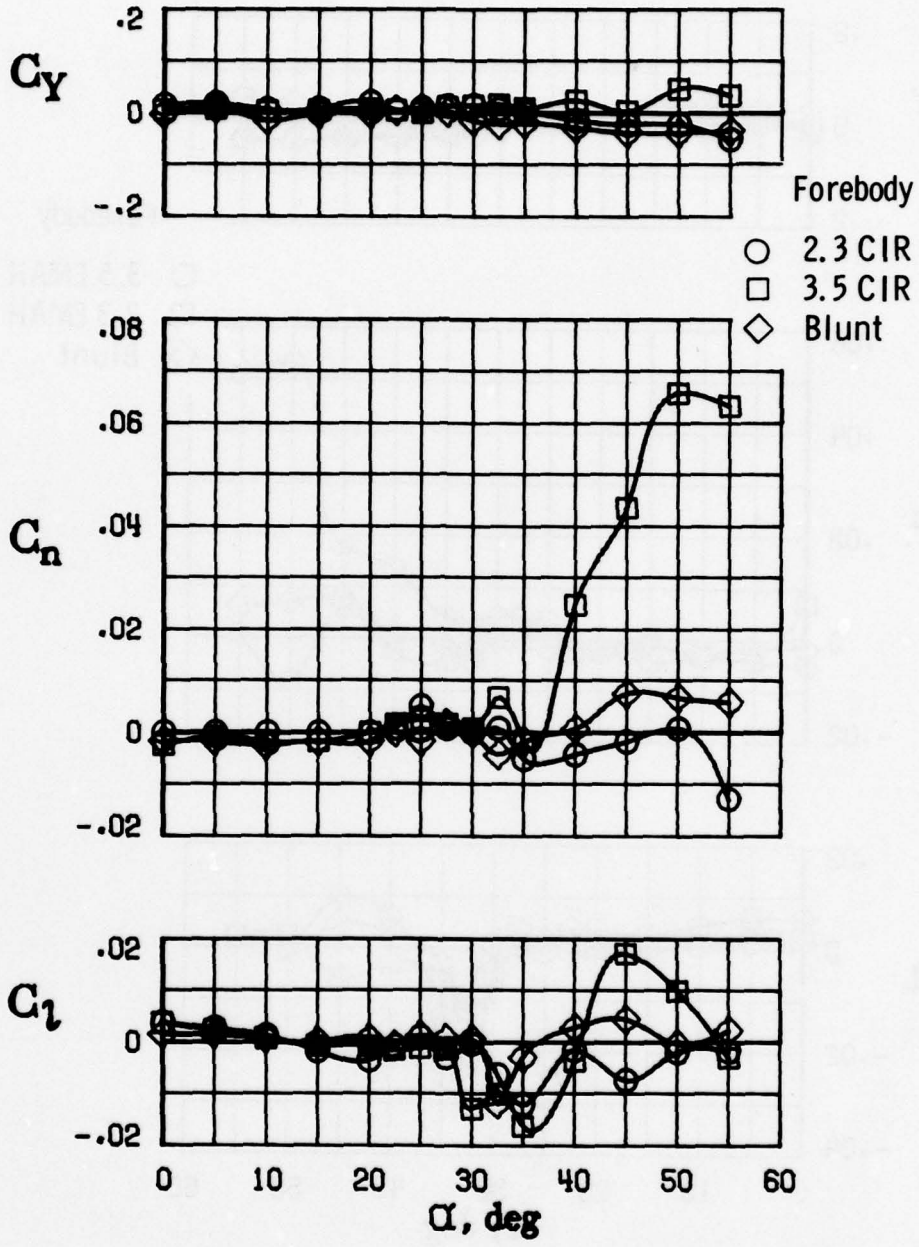

(a) CIR cross section.

Figure 11.- Effect of forebody fineness ratio on lateral-directional aerodynamic symmetry; $\beta = 0^\circ$; $\delta_h = 0^\circ$; inlet cowl 12° down.

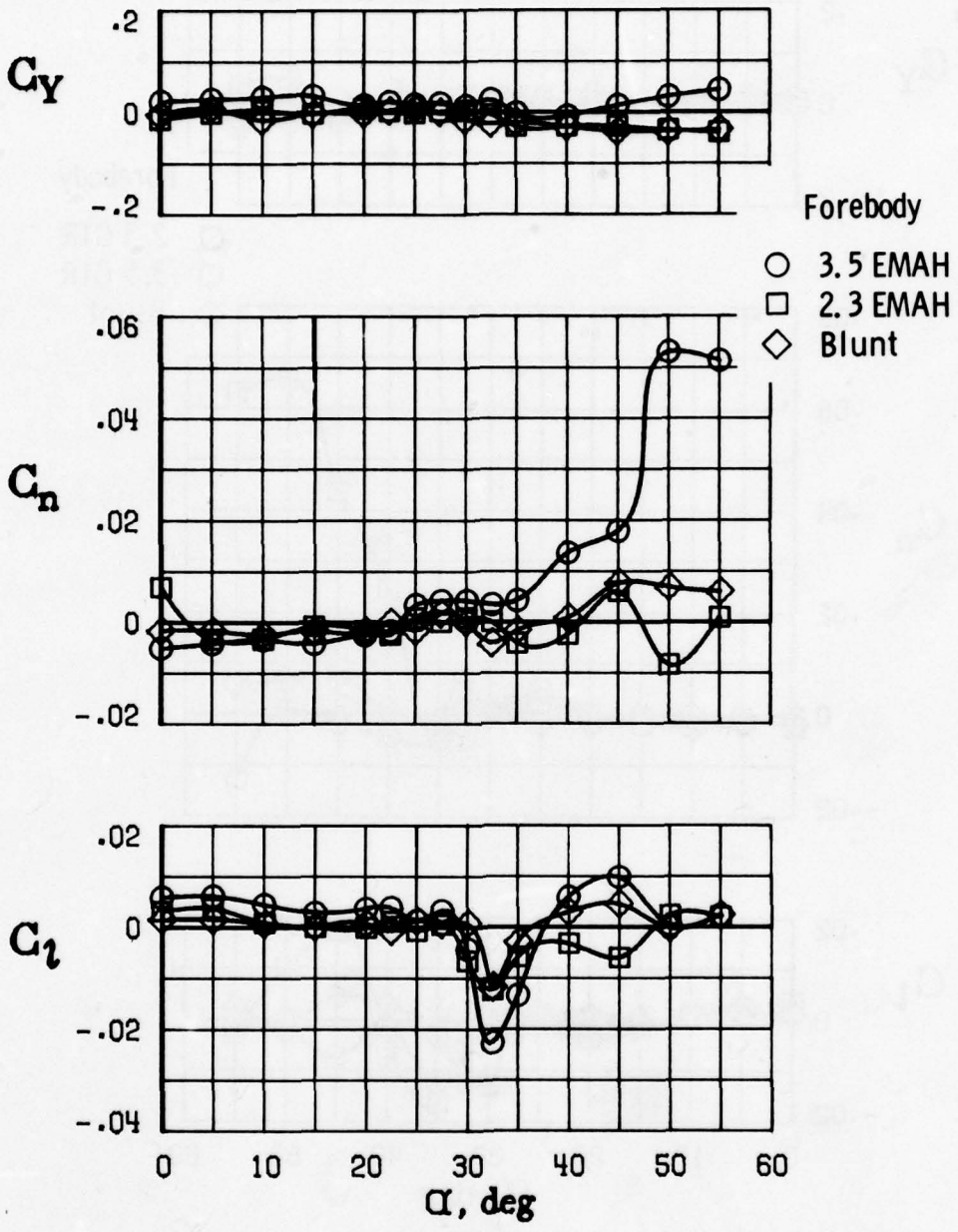

(b) EMAH cross section.

Figure 11.- Concluded.

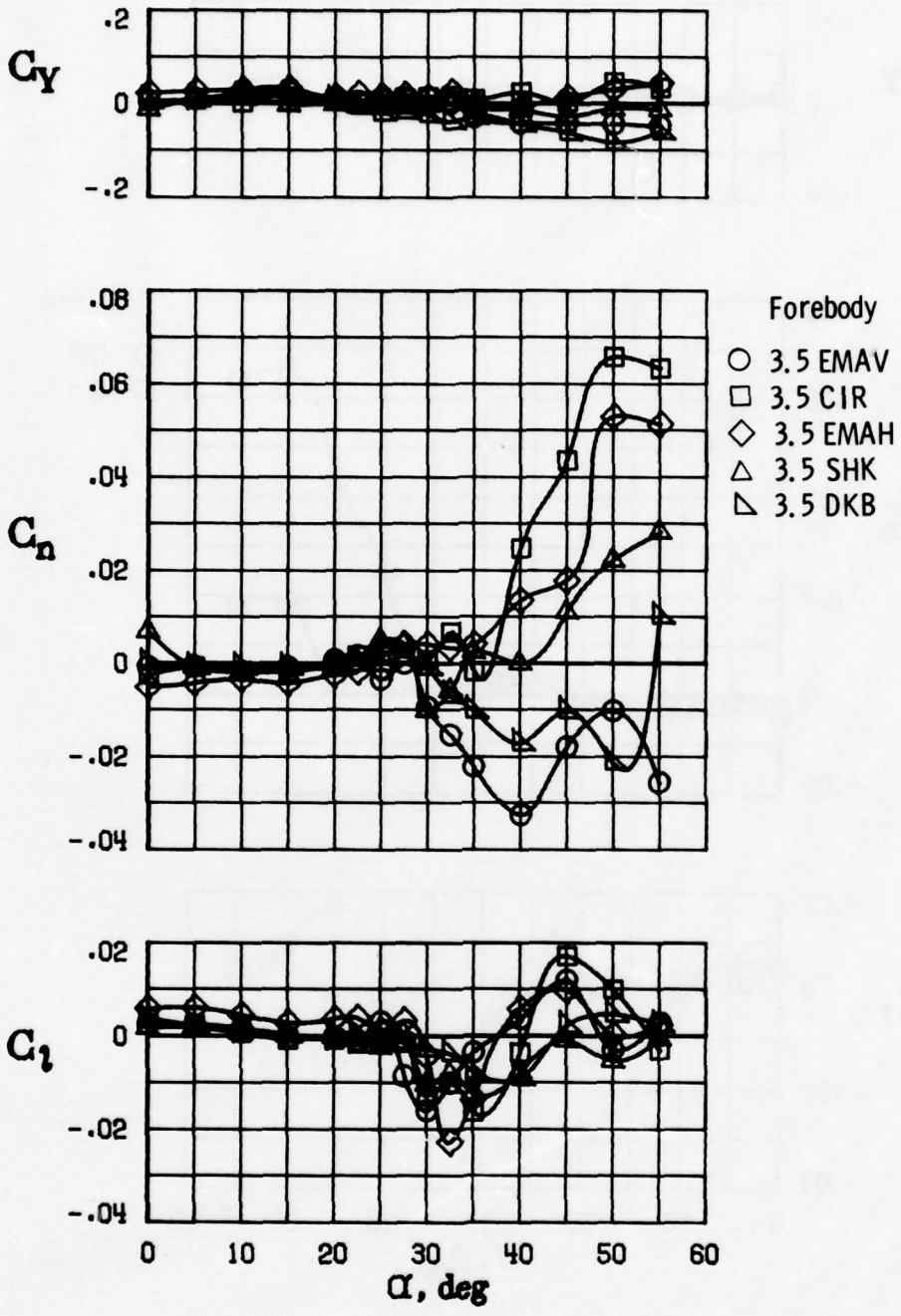

Figure 12.- Effect of forebody cross-sectional shape on lateral-directional aerodynamic symmetry; $\beta = 0^{\circ}$; 3.5 fineness ratio; $\delta_h = 0^{\circ}$; inlet cowl 12° down.

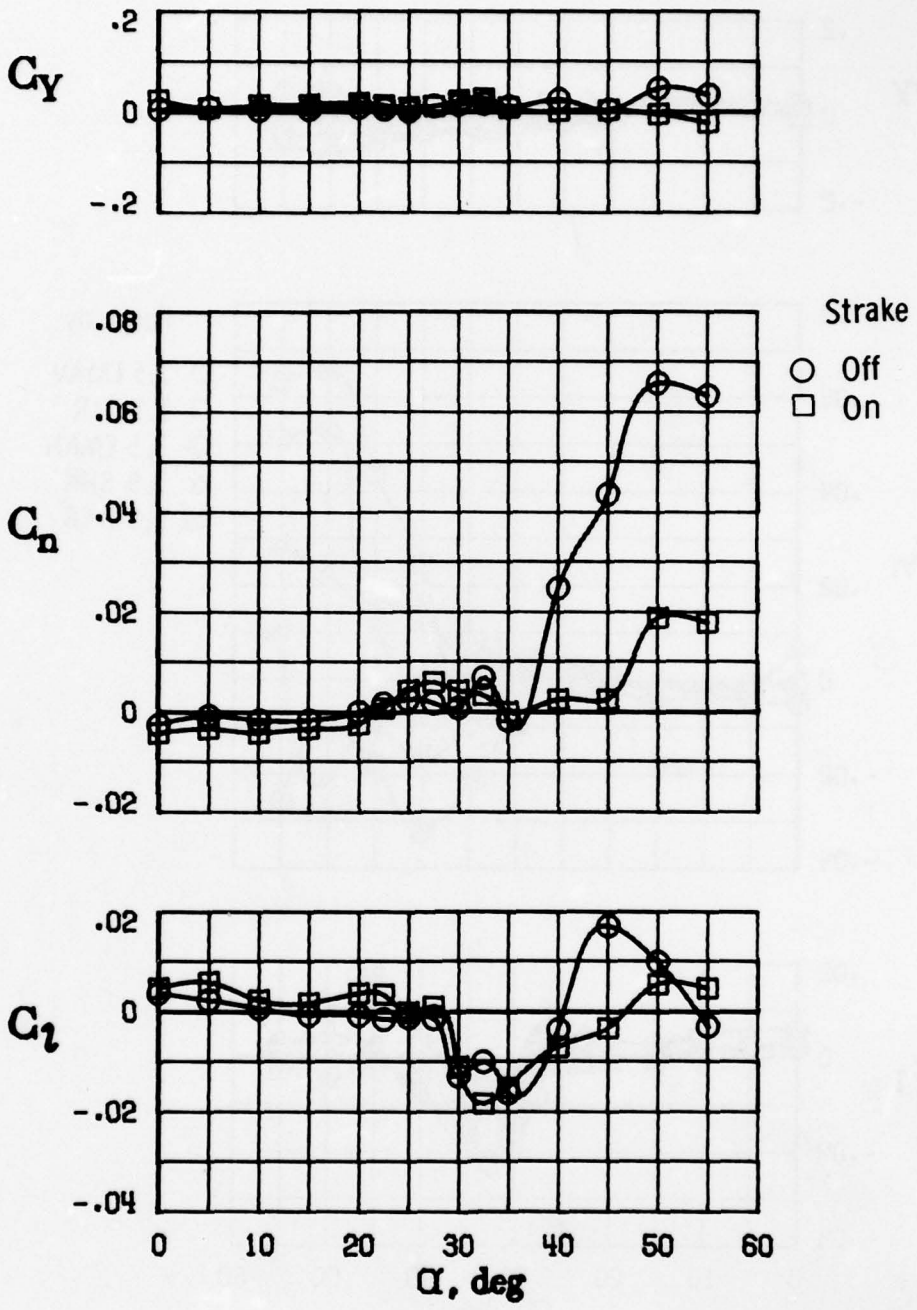

(a) 3.5 CIR forebody.

Figure 13.- Effect of fuselage forebody strakes on lateral-directional aerodynamic symmetry; $\beta = 0^{\circ}$; 3.5 fineness ratio; $\delta_h = 0^{\circ}$; inlet cowl 12° down.

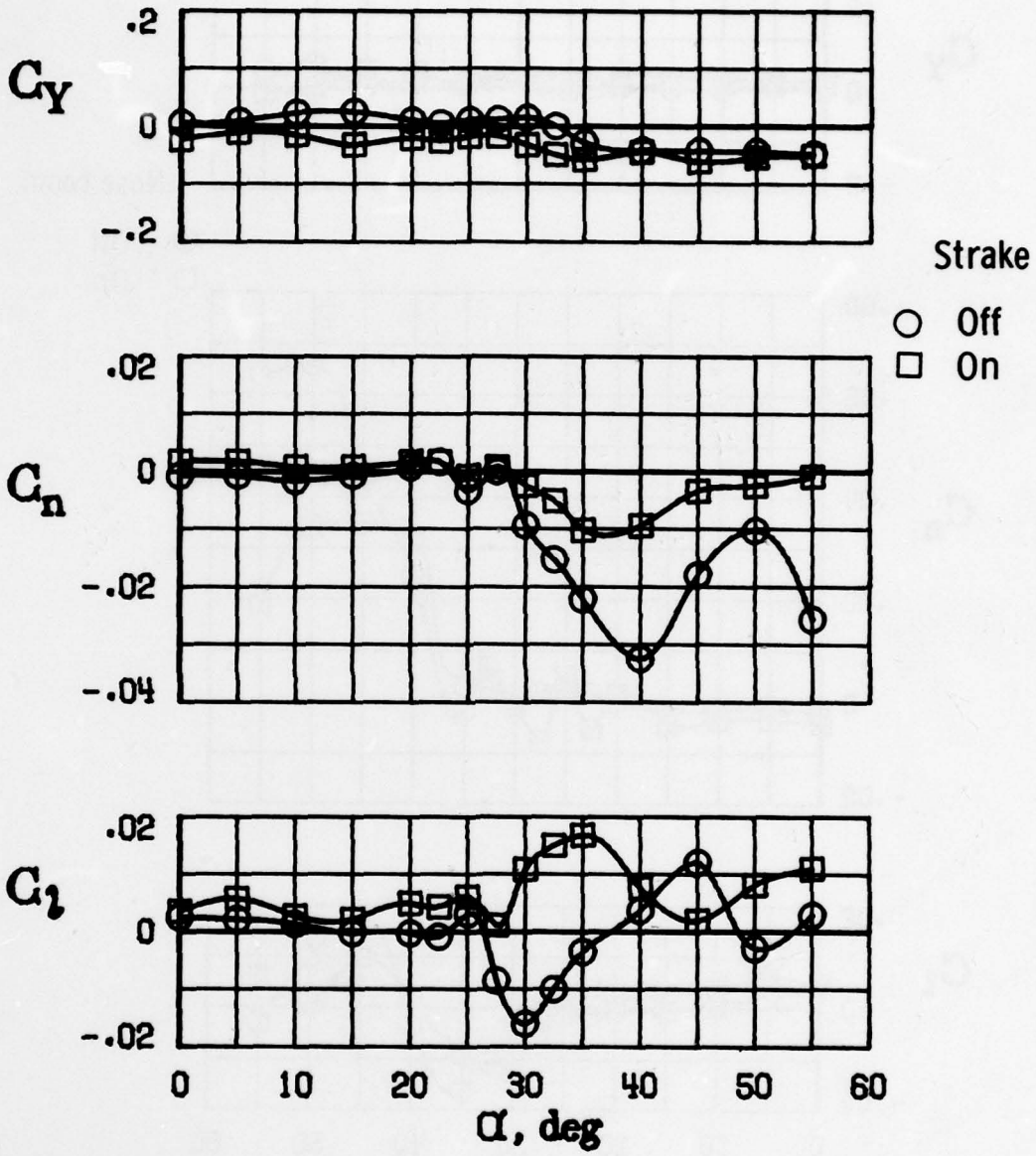

(b) 3.5 EMAV forebody.

Figure 13.- Concluded.

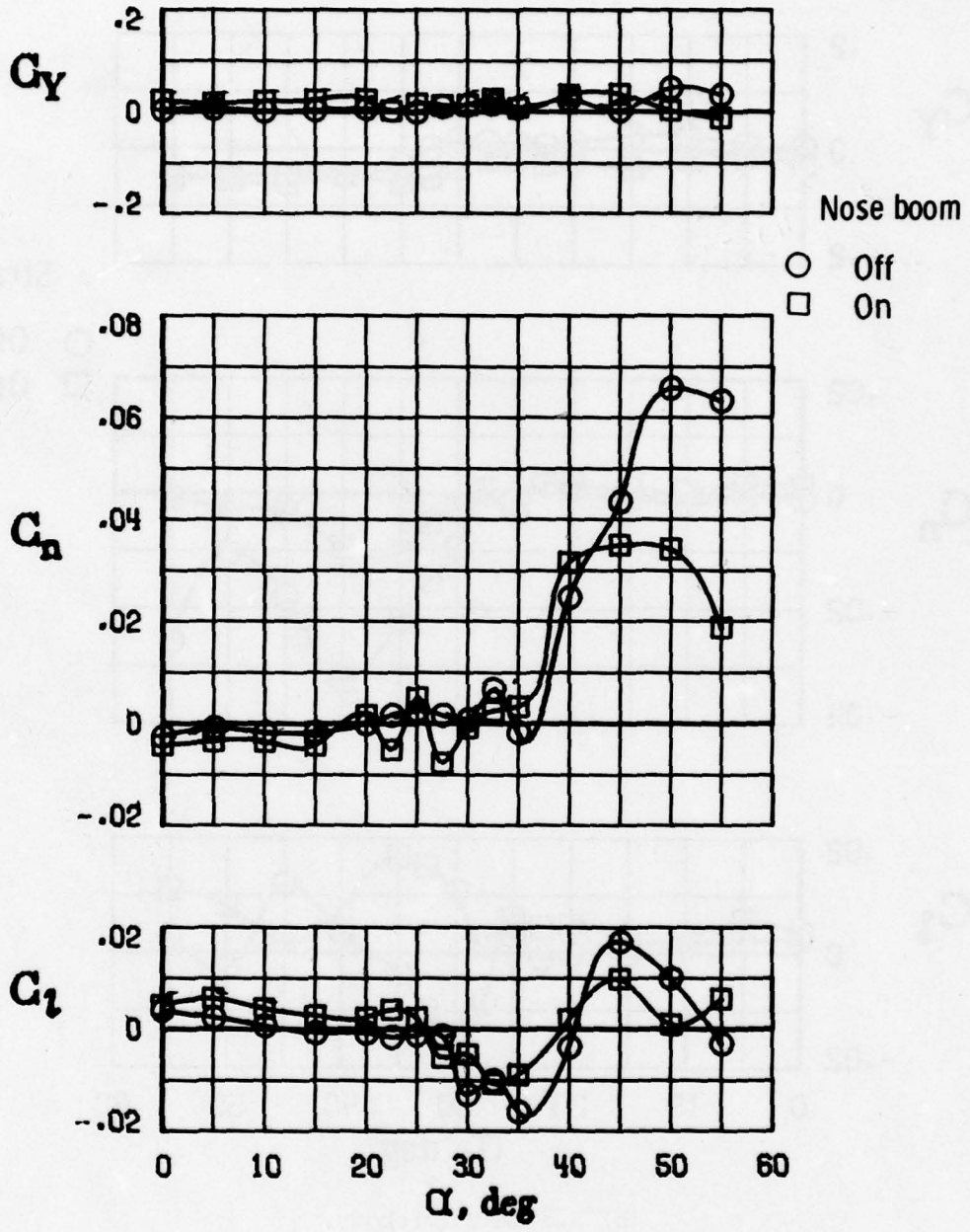

Figure 14.- Effect of nose boom on lateral-directional aerodynamic symmetry; $\beta = 0^{\circ}$; 3.5 CIR forebody; $\delta_h = 0^{\circ}$; inlet cowl 12° down.

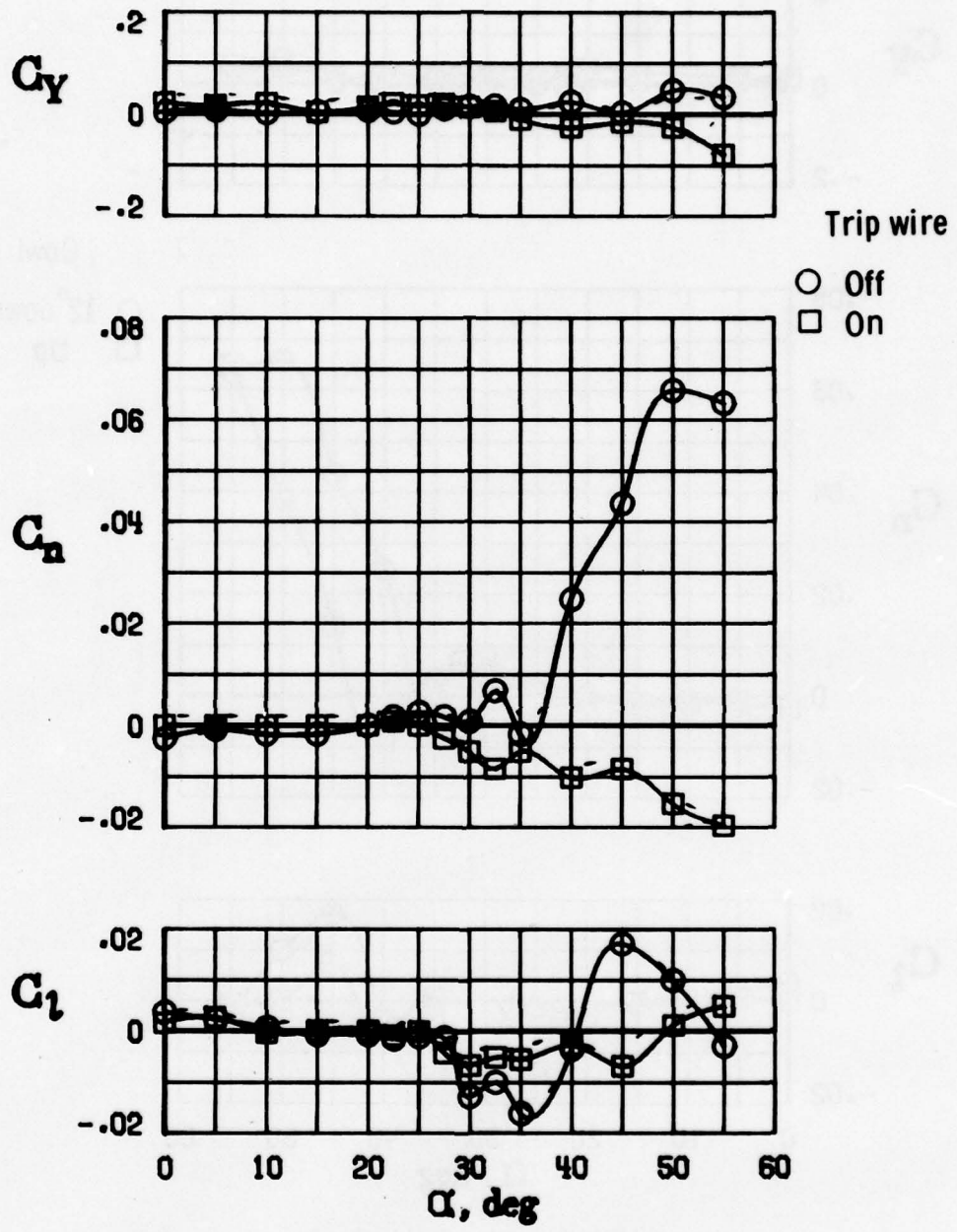

Figure 15.- Effect of boudary-layer helical trip wire on lateral-directional aerodynamic symmetry; $\beta = 0^\circ$; 3.5 CIR forebody; $\delta_h = 0^\circ$; inlet cowl 12° down.

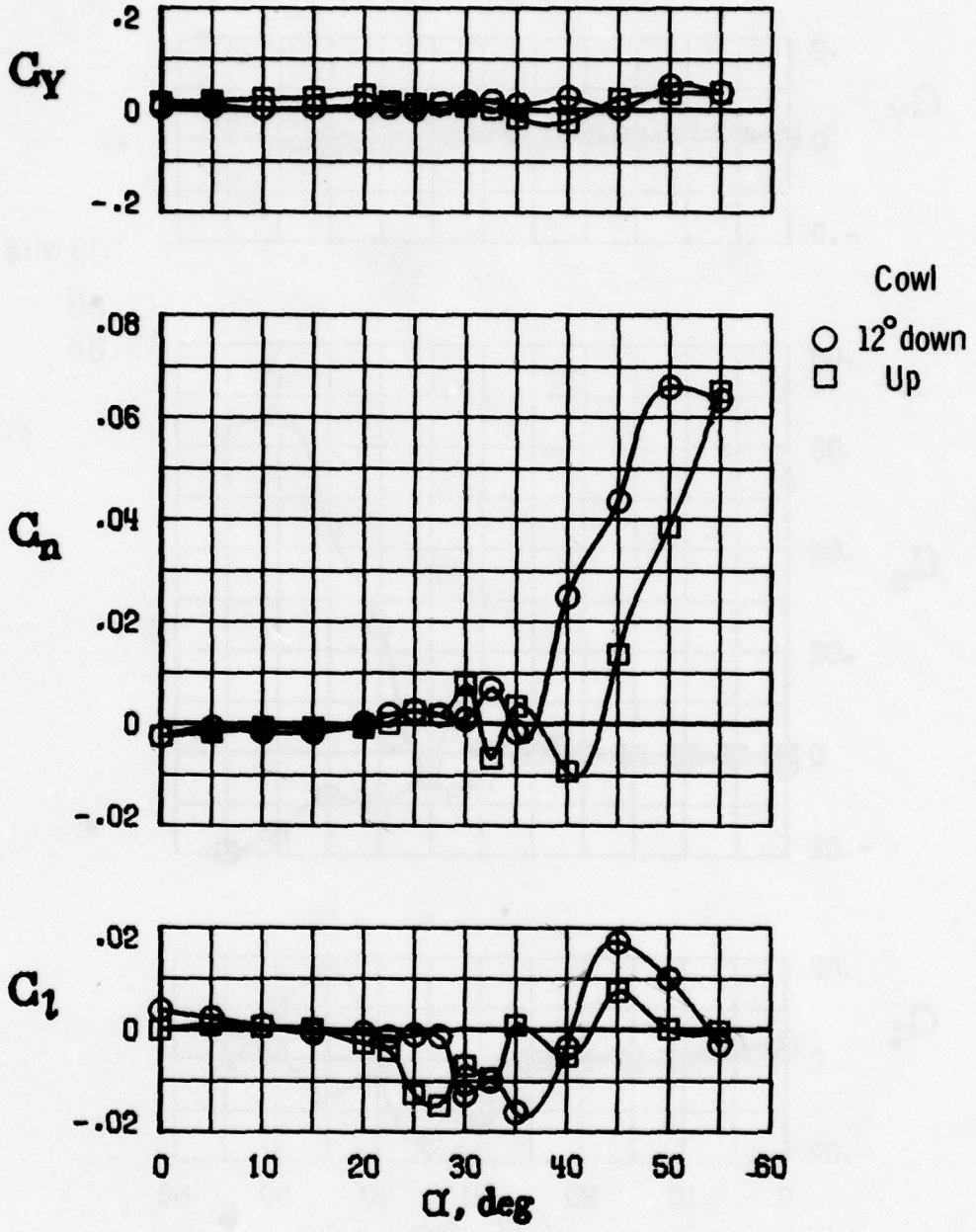

(a) 3.5 CIR forebody.

Figure 16.- Effect of engine inlet cowl deflection on lateral-directional aerodynamic symmetry; $\beta = 0^\circ$; 3.5 fineness ratio; $\delta_h = 0^\circ$.

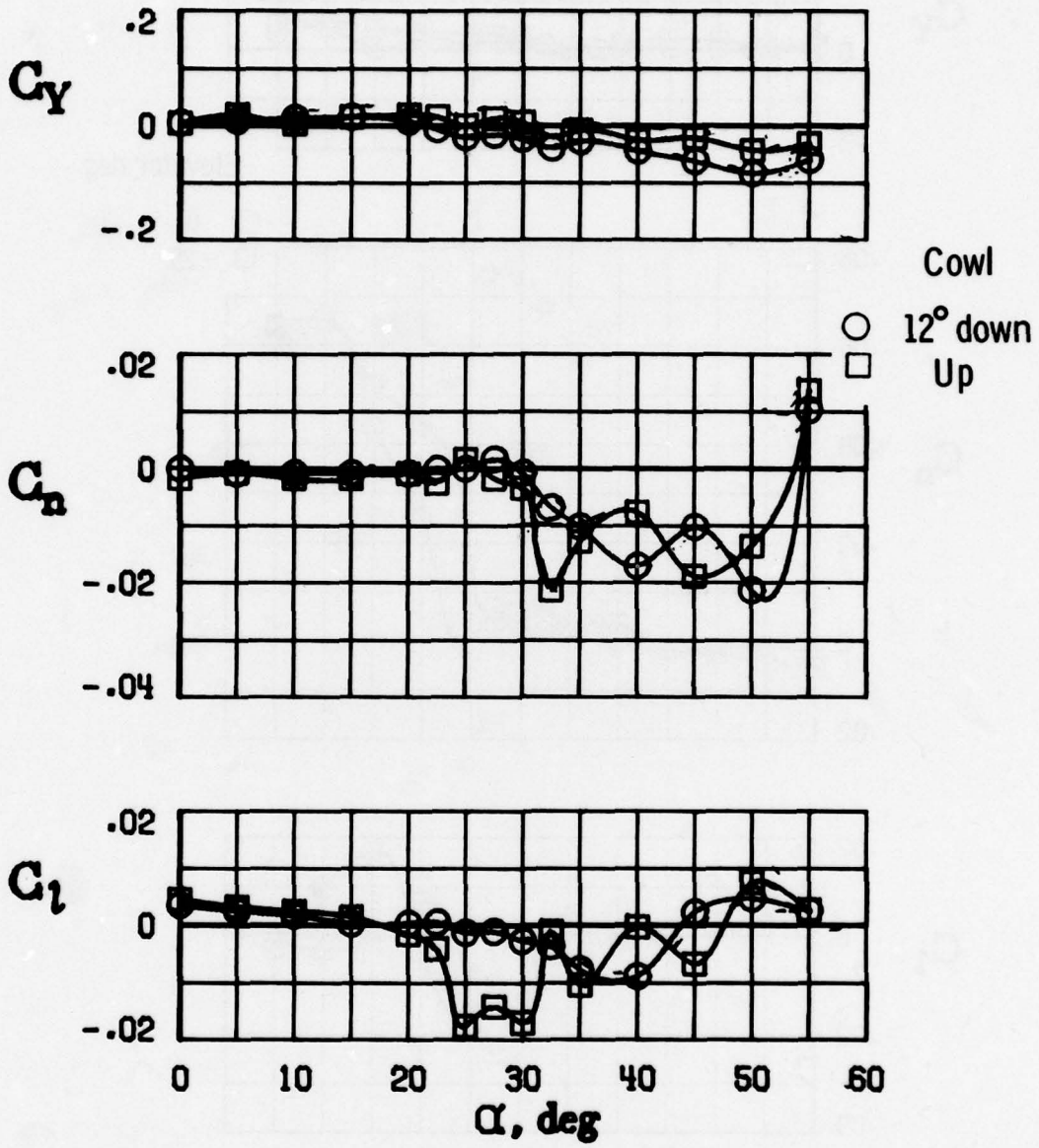

(b) 3.5 DKB forebody.

Figure 16.- Concluded.

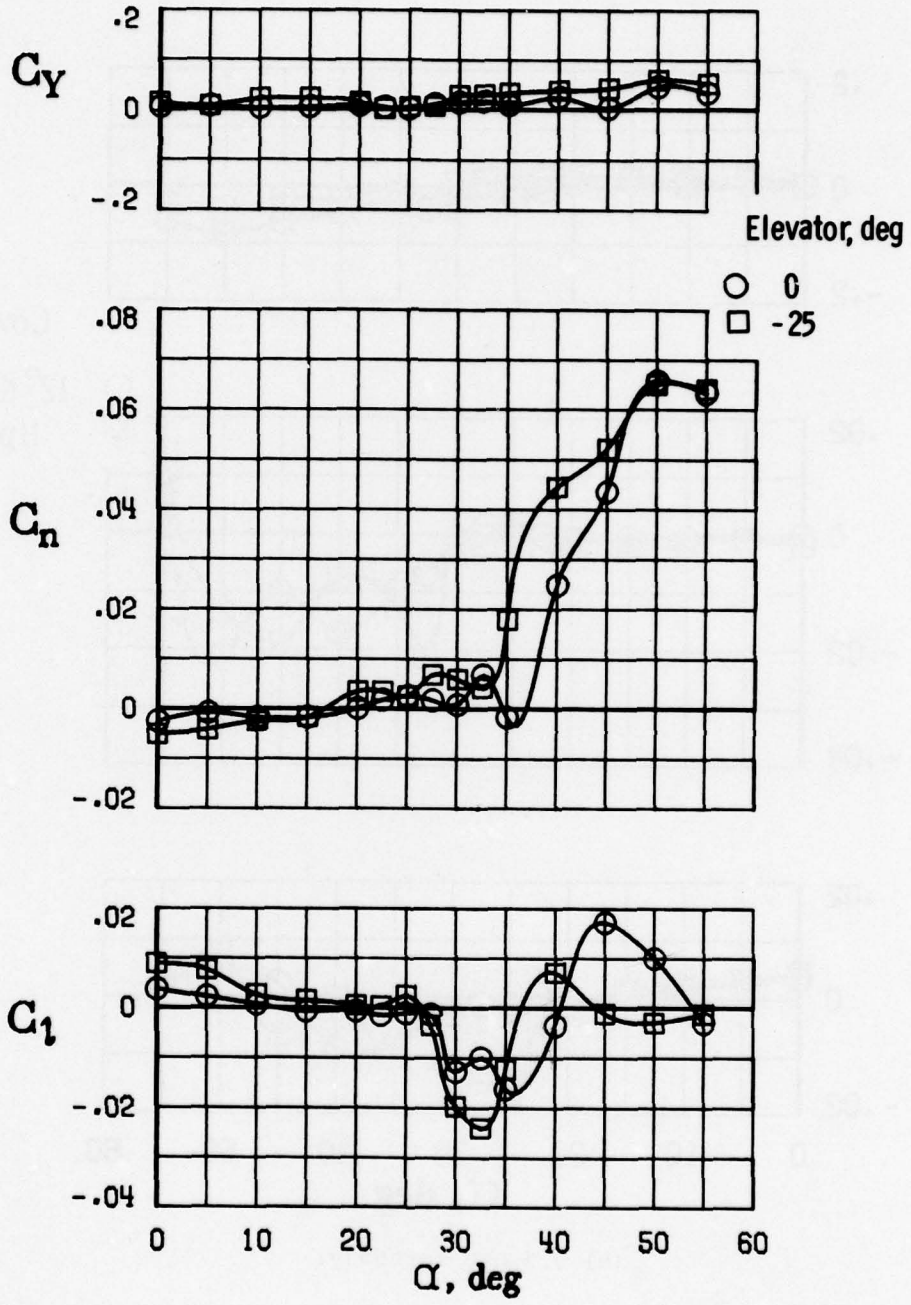

Figure 17.- Effect of elevator deflection on lateral-directional aerodynamic symmetry; $\beta = 0^{\circ}$; 3.5 CIR forebody; inlet cowl 12° down.

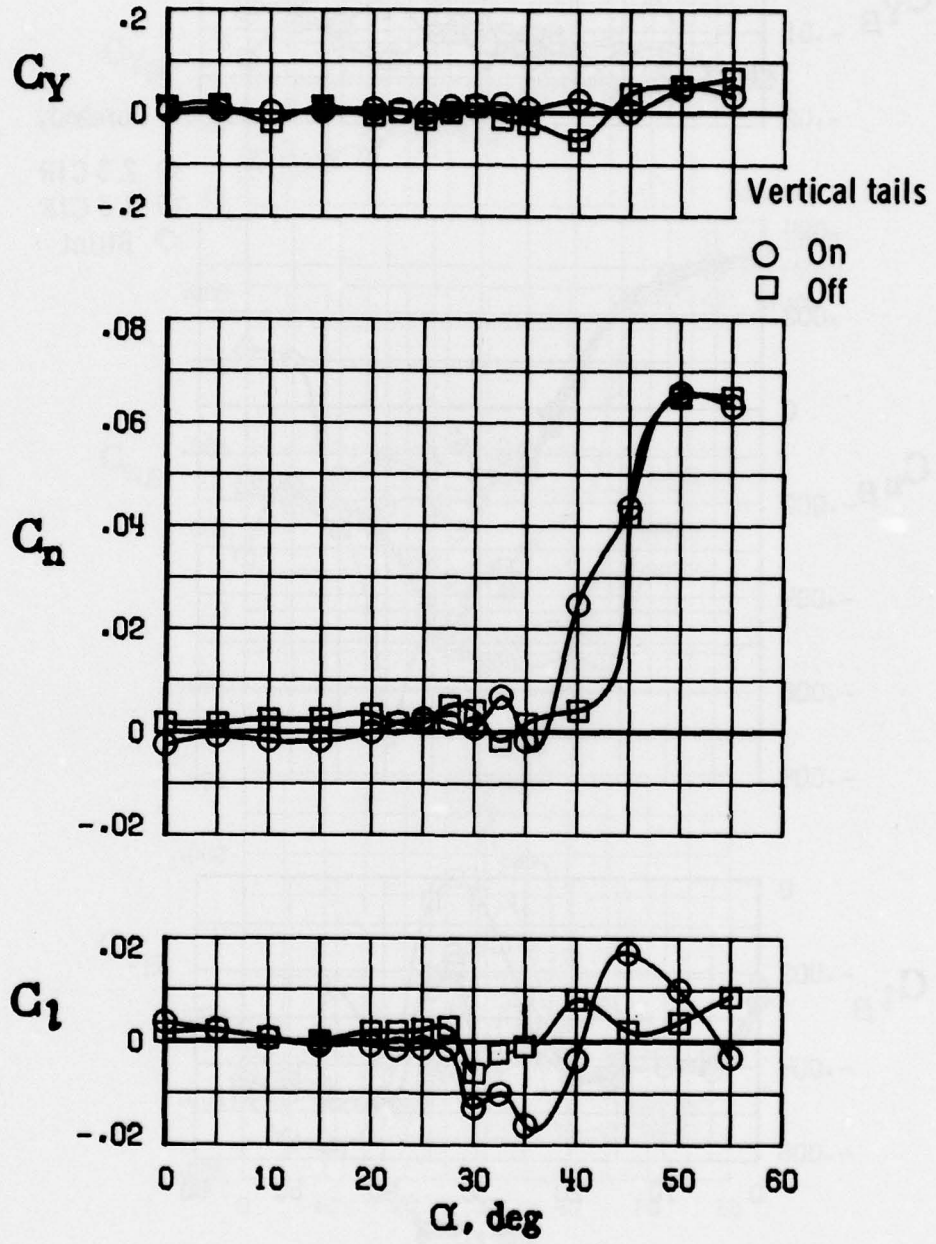

Figure 18.- Effect of vertical tails on aerodynamic lateral-directional symmetry; $\beta = 0^\circ$; 3.5 CIR forebody; $\delta_h = 0^\circ$; inlet cowl 12° down.

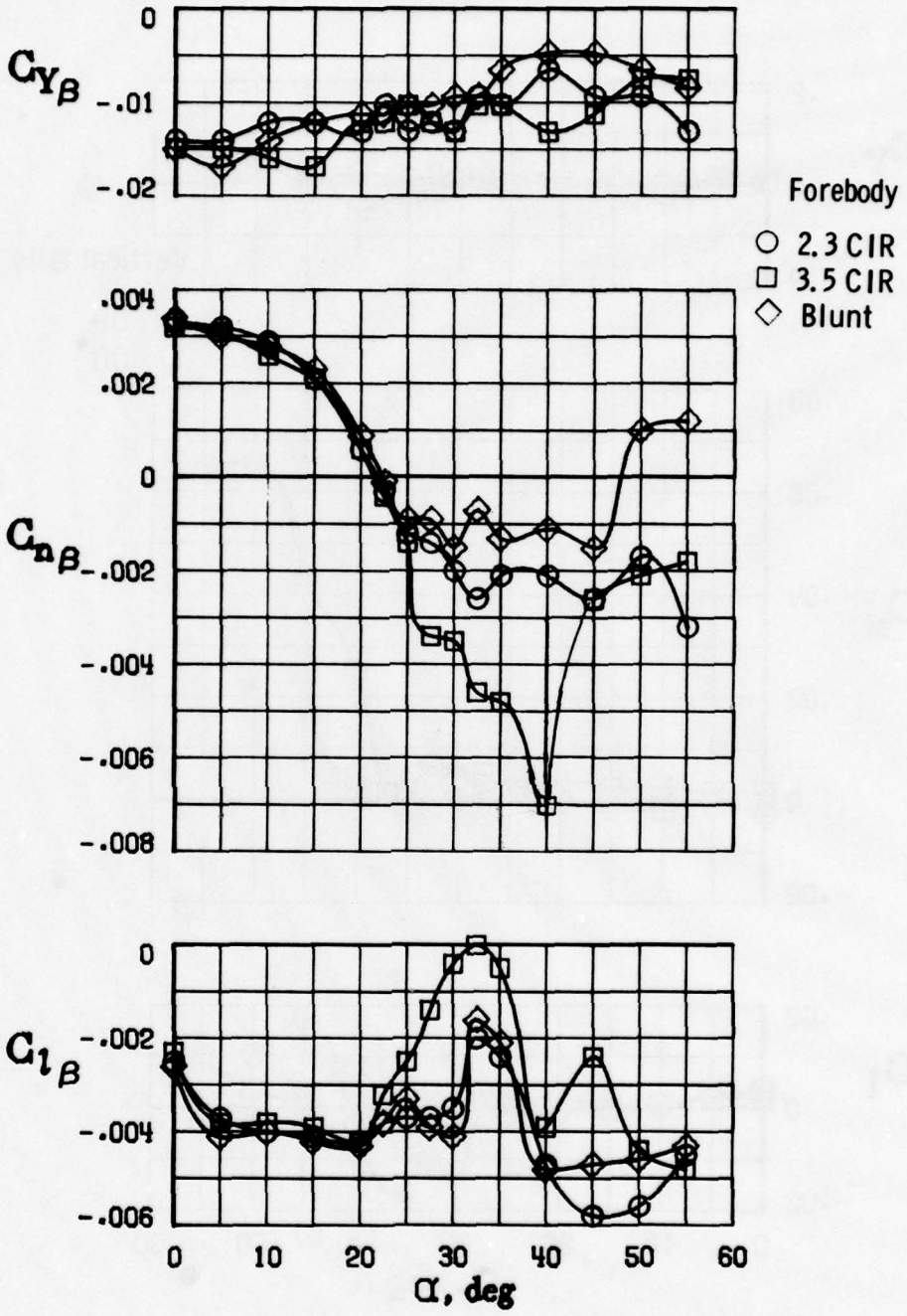

(a) CIR cross section.

Figure 19.- Effect of forebody fineness ratio on lateral-directional stability; $\delta_h = 0^\circ$; inlet cowl 12° down.

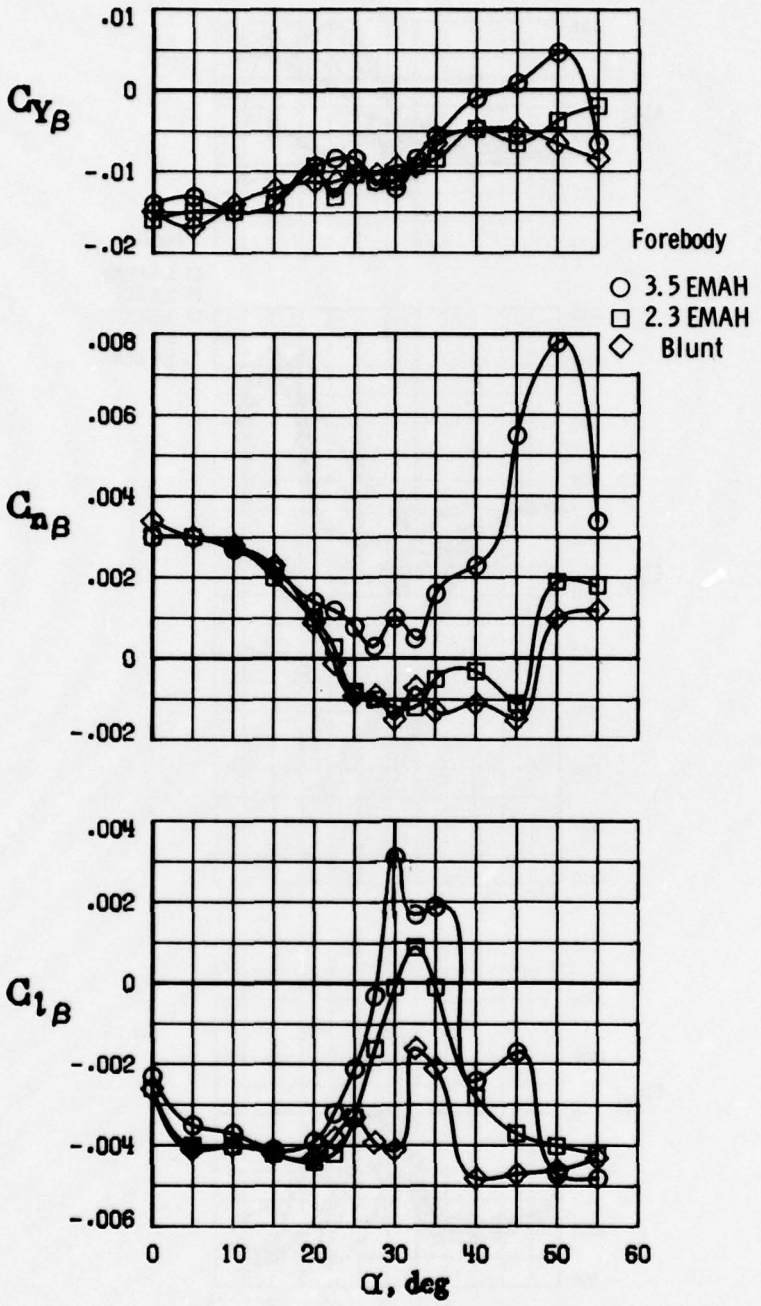

(b) EMAH cross section.

Figure 19.- Concluded.

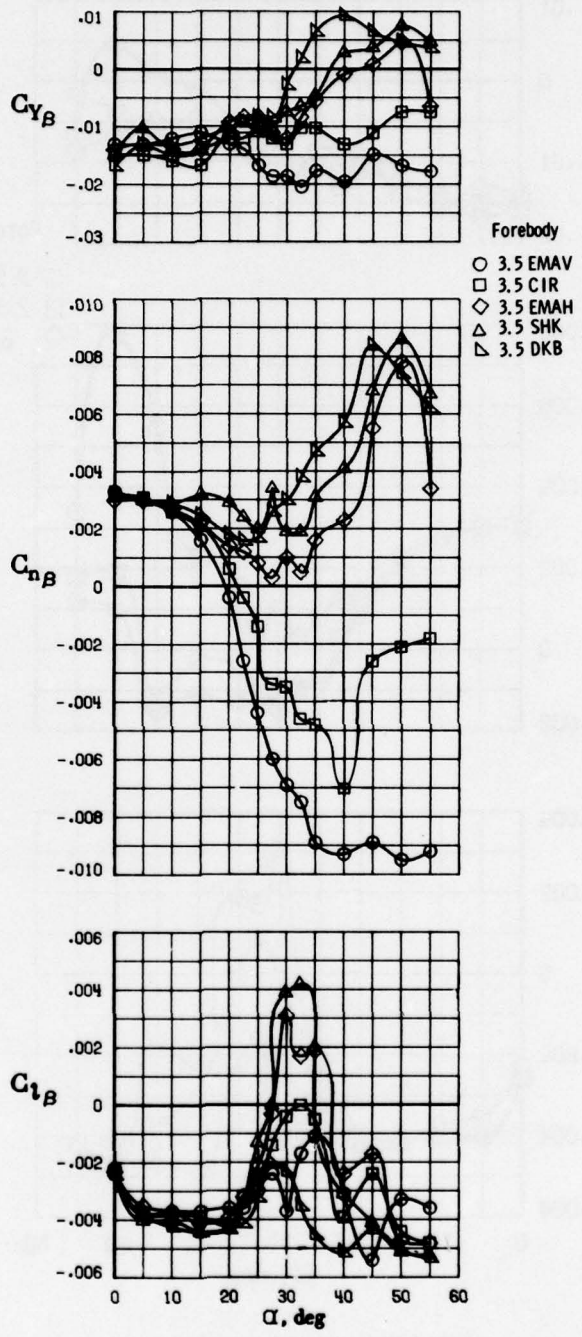

Figure 20.- Effect of forebody cross-sectional shape on lateral-directional stability for 3.5 fineness ratio; $\delta_h = 0^o$; inlet cowl 12^o down.

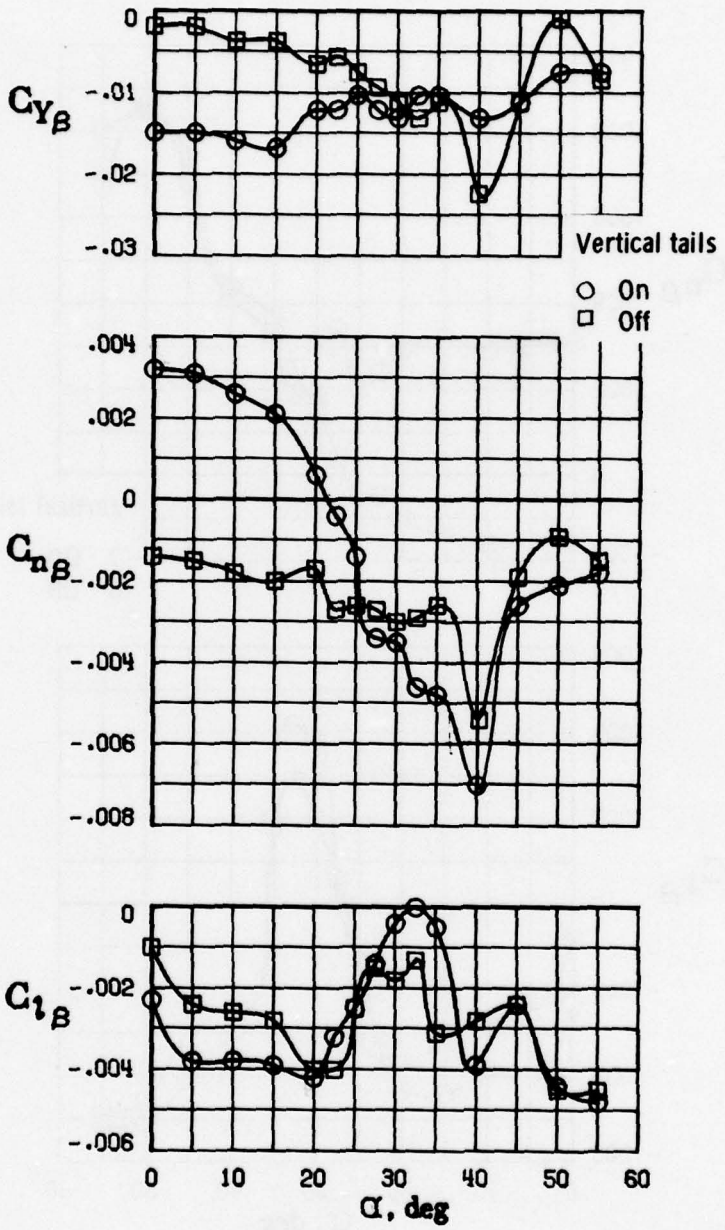

(a) 3.5 CIR forebody.

Figure 21.- Effect of vertical tails on lateral-directional stability for 3.5 fineness ratio forebodies; $\delta_h = 0^\circ$; inlet cowl 12° down.

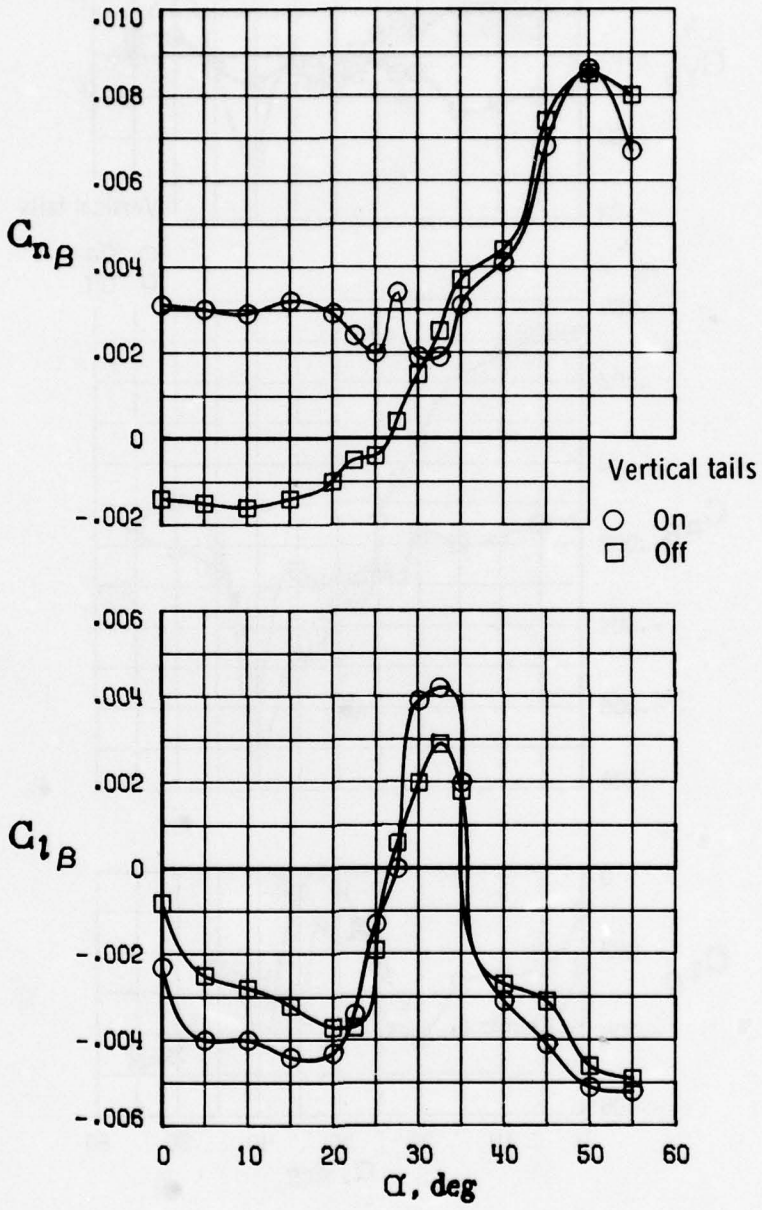

(b) 3.5 SHK forebody.

Figure 21.- Continued.

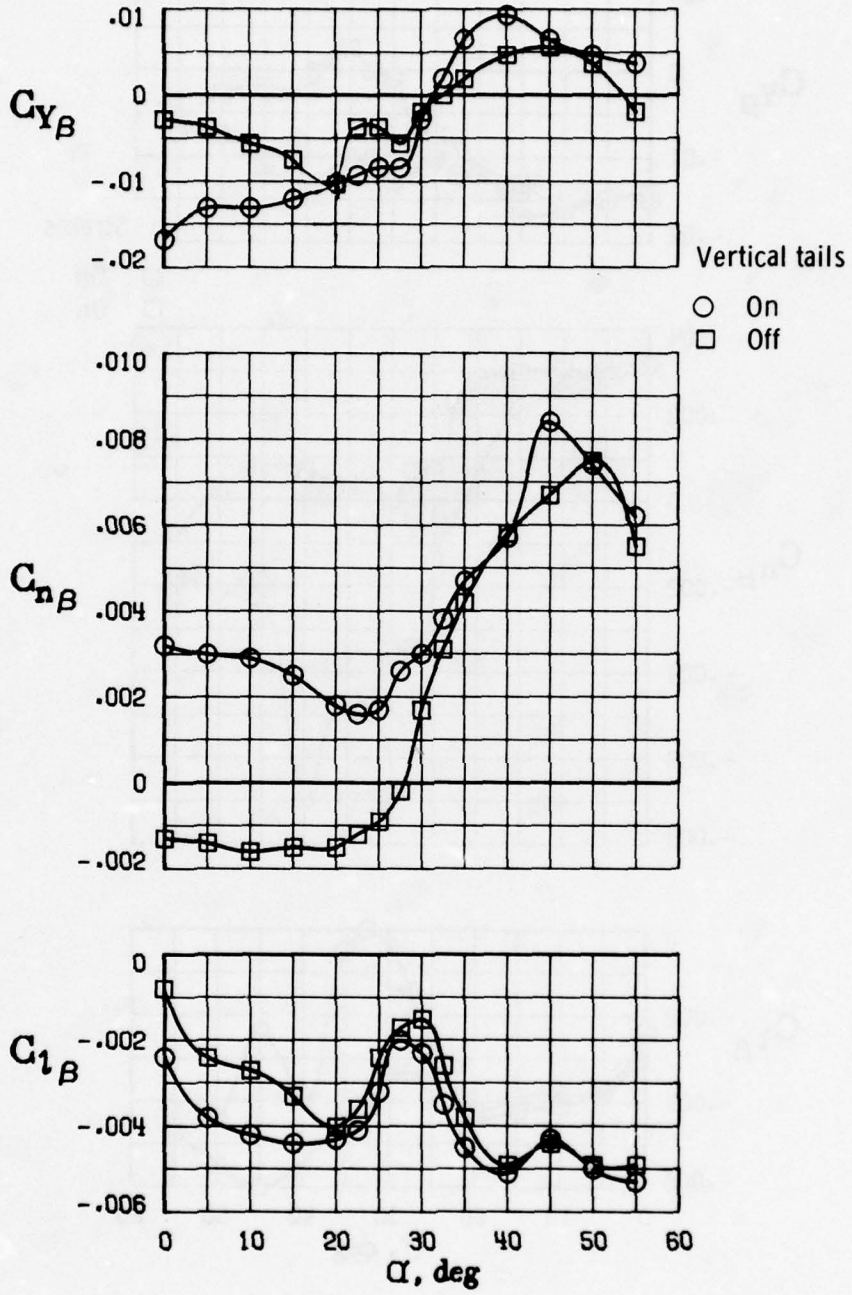

(c) 3.5 DKB forebody.

Figure 21.- Concluded.

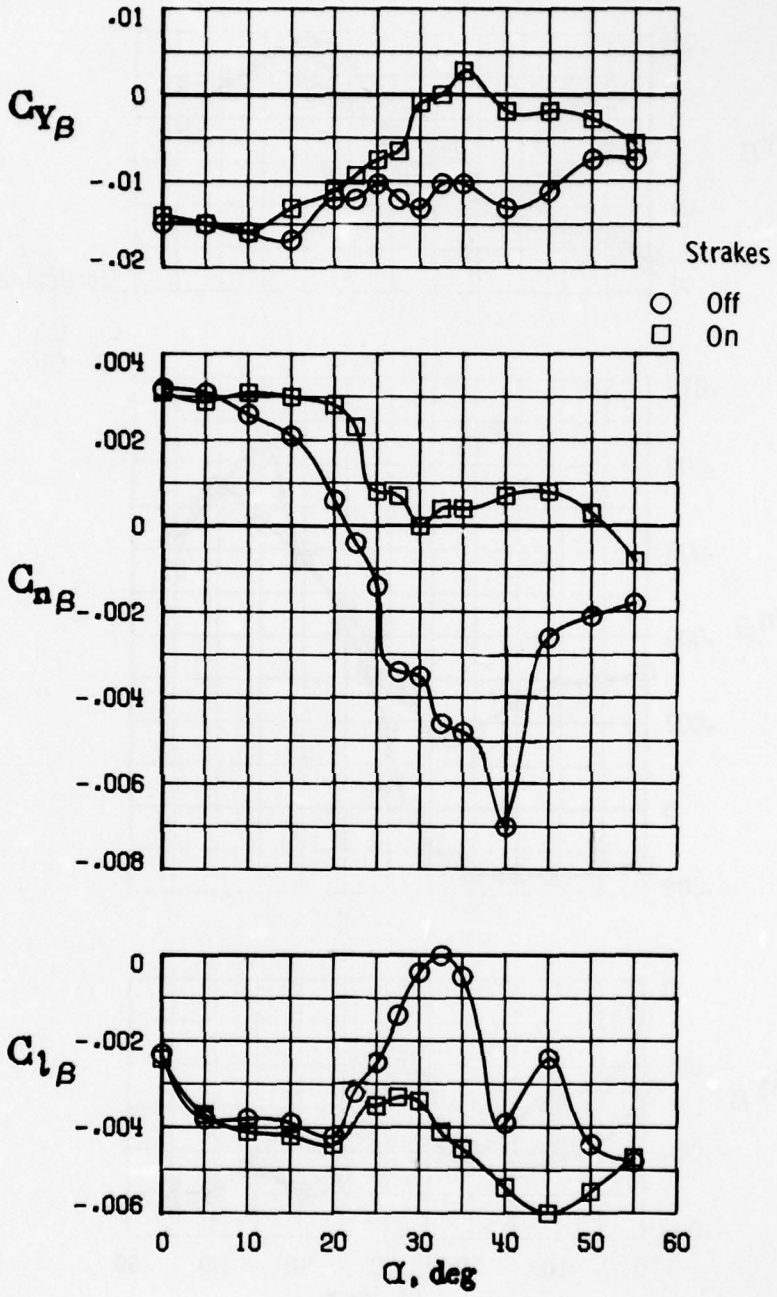

(a) 3.5 CIR forebody with and without strakes.

Figure 22.- Effect of fuselage forebody strakes and vertical tails on lateral-directional stability for several forebody designs; $\delta_h = 0^\circ$; inlet cowl 12° down.

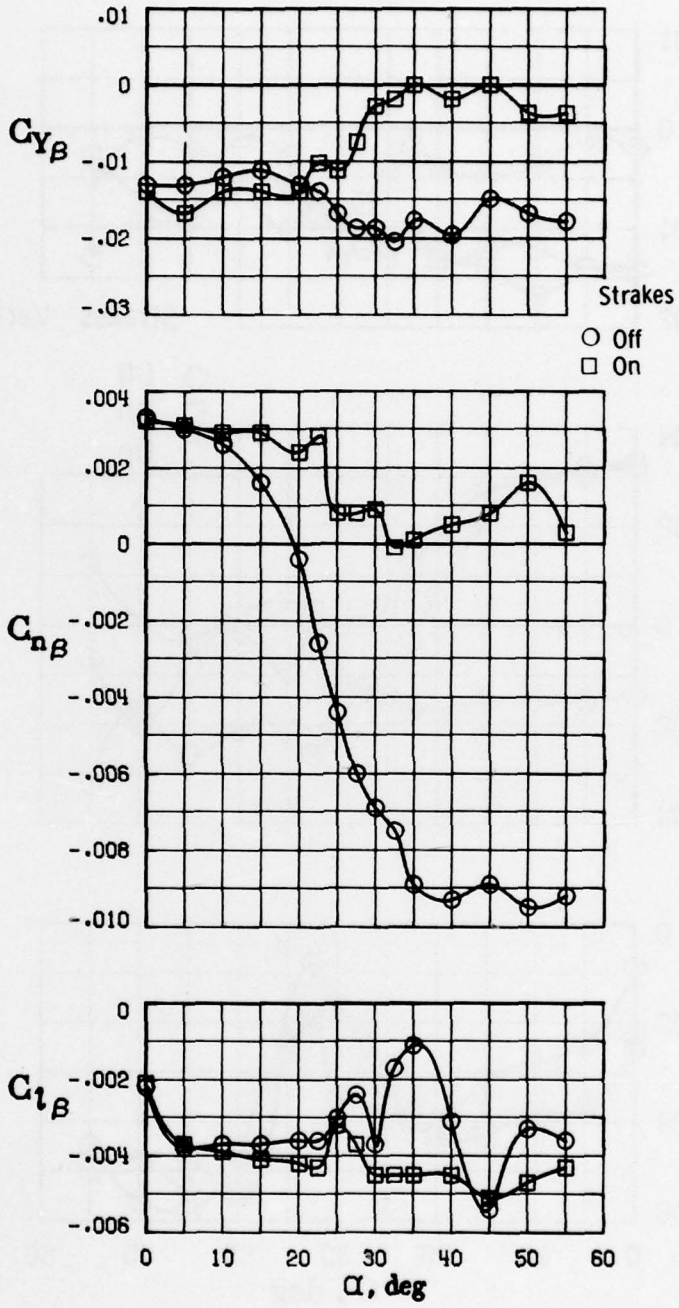

(b) 3.5 EMAV forebody with and without strakes.

Figure 22.- Continued.

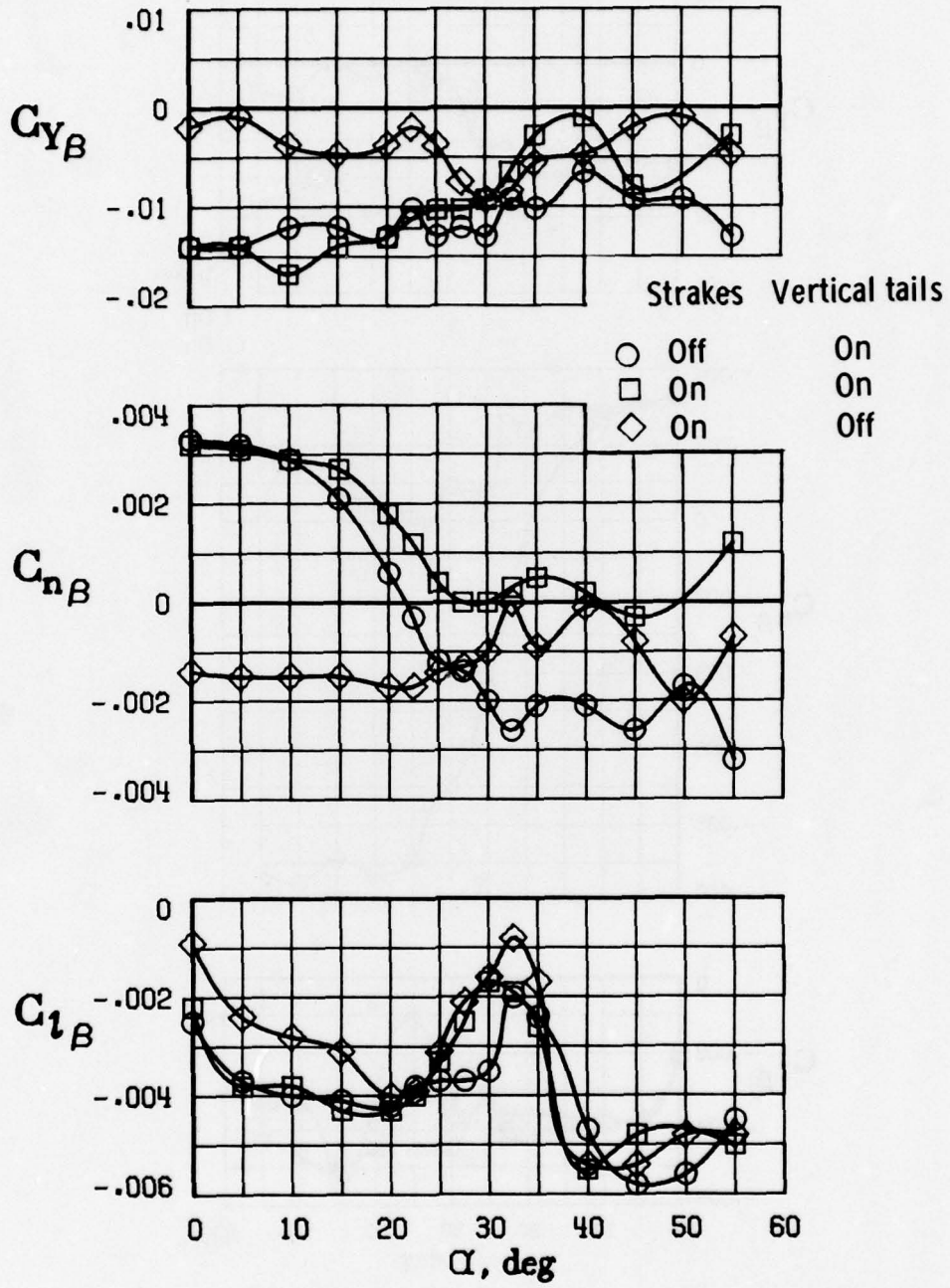

(c) 2.3 CIR forebody with and without strakes and vertical tails.

Figure 22.- Continued.

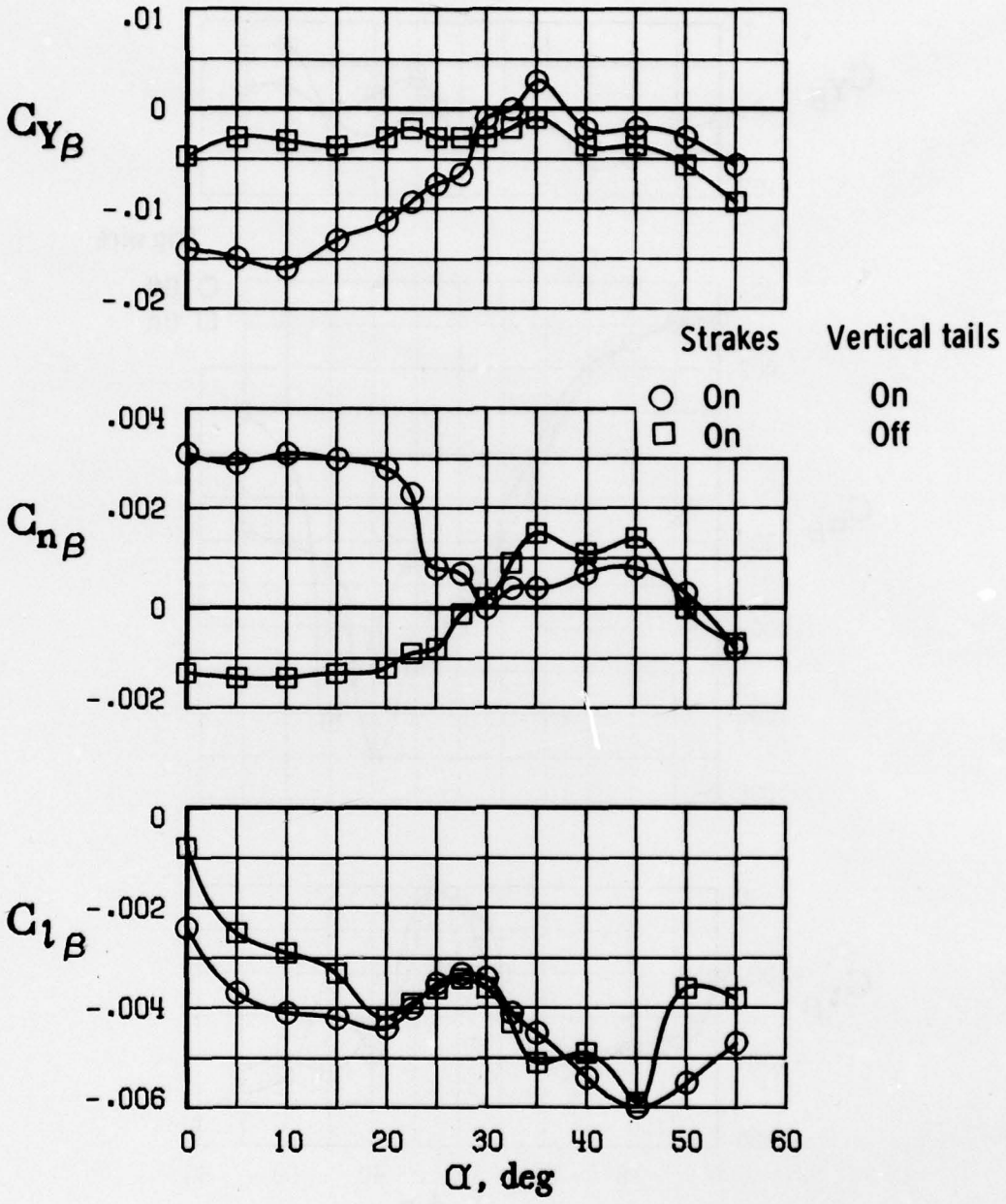

(d) 3.5 CIR forebody with nose strakes and with and without vertical tails.

Figure 22.- Concluded.

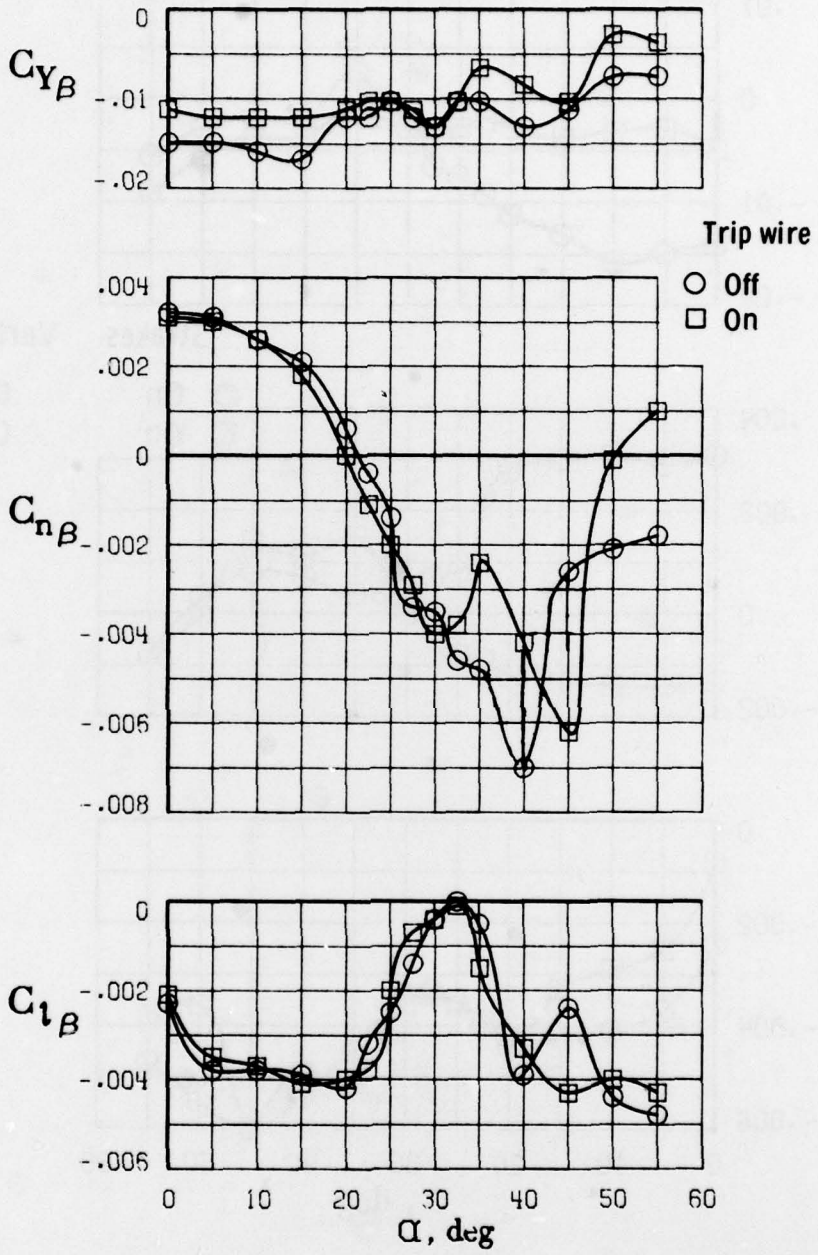

Figure 23.- Effect of boundary-layer helical trip wire on lateral-directional stability for 3.5 CIR forebody; $\delta_h = 0^o$; inlet cowl 12^o down.

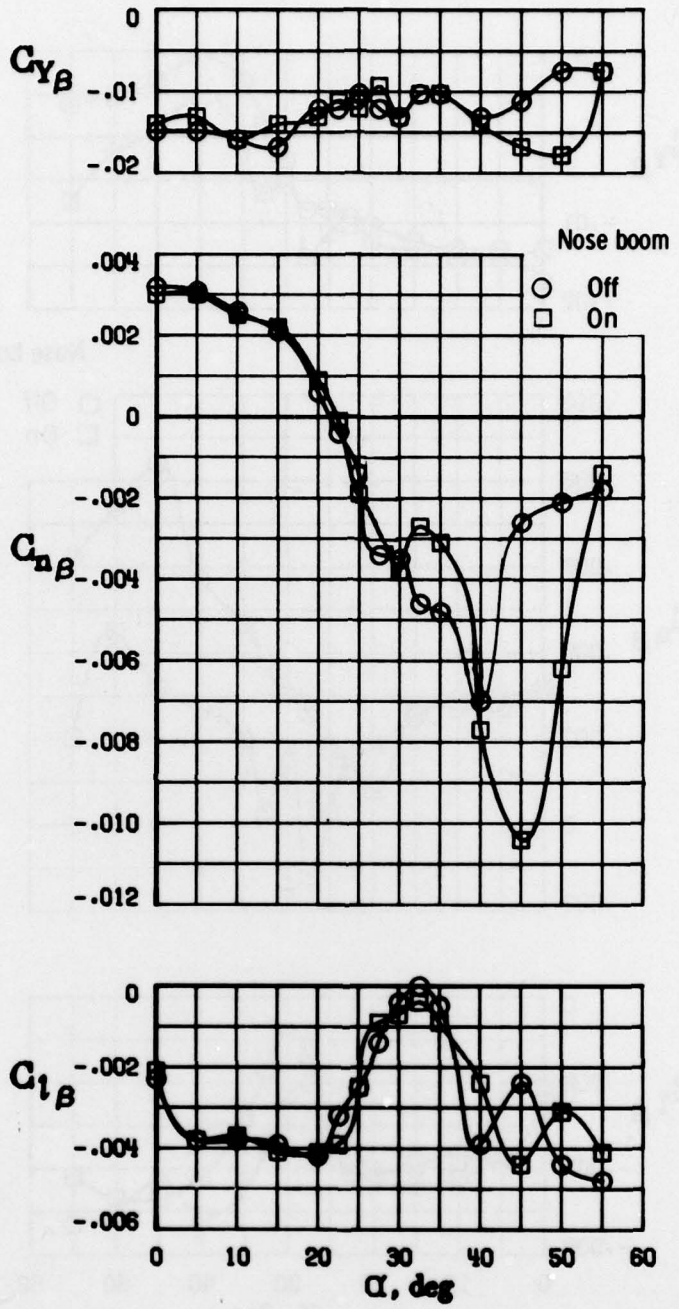

(a) 3.5 CIR forebody.

Figure 24.- Effect of nose boom on lateral-directional stability for two 3.5 fineness ratio forebodies; $\delta_h = 0^\circ$; inlet cowl 12° down.

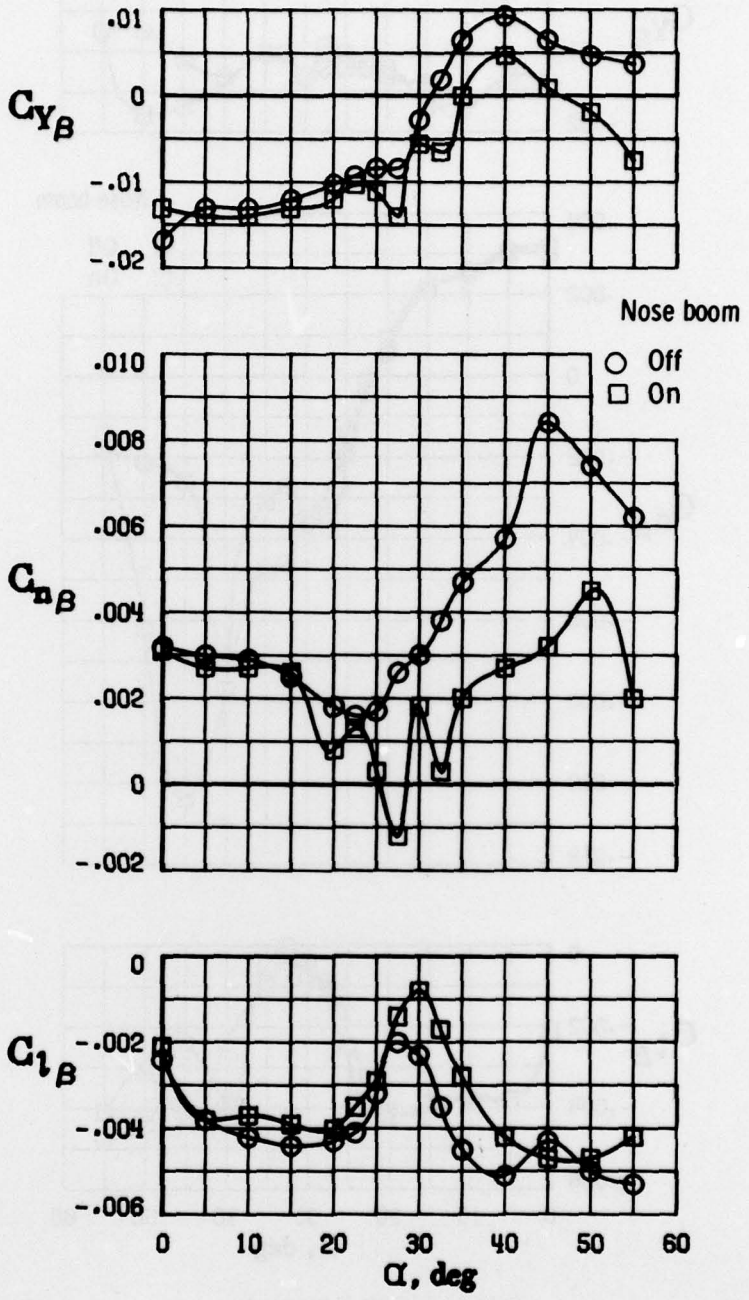

(b) 3.5 DKB forebody.

Figure 24.- Concluded.

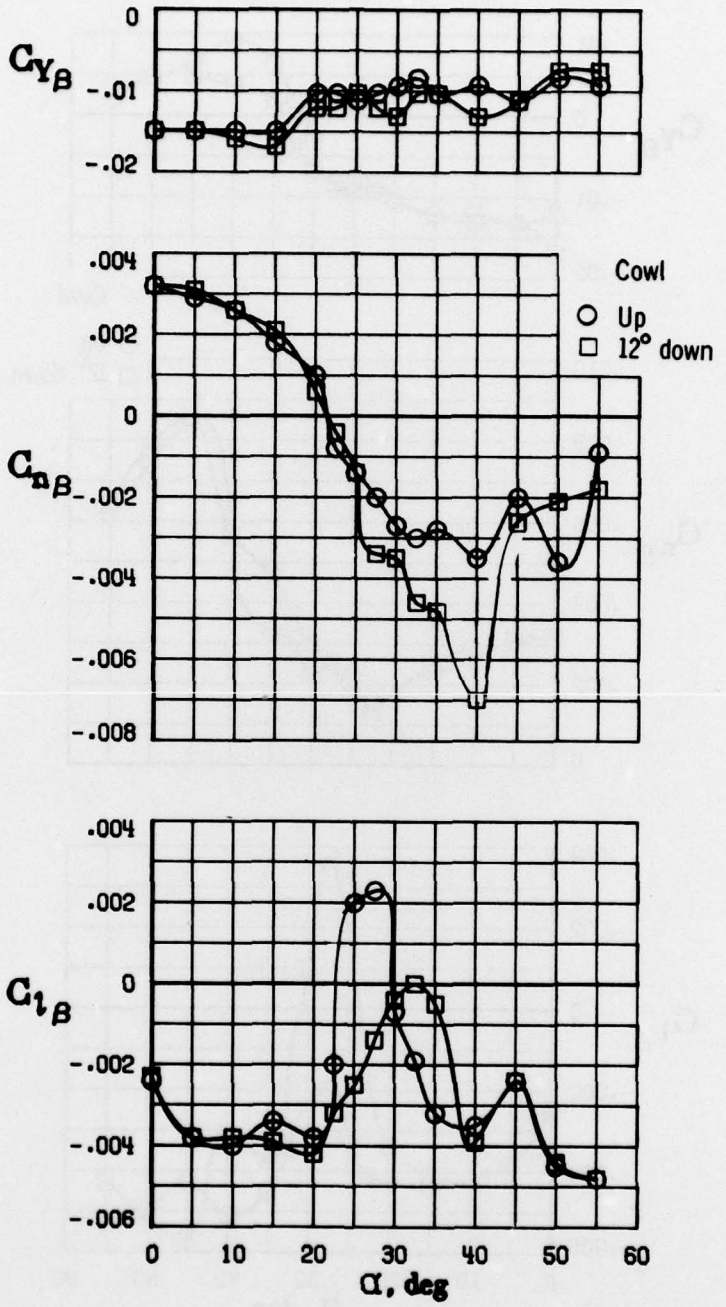

(a) 3.5 CIR forebody.

Figure 25.- Effect of engine inlet cowl deflection on lateral-directional stability for two 3.5 fineness ratio forebodies; $\delta_h = 0^\circ$.

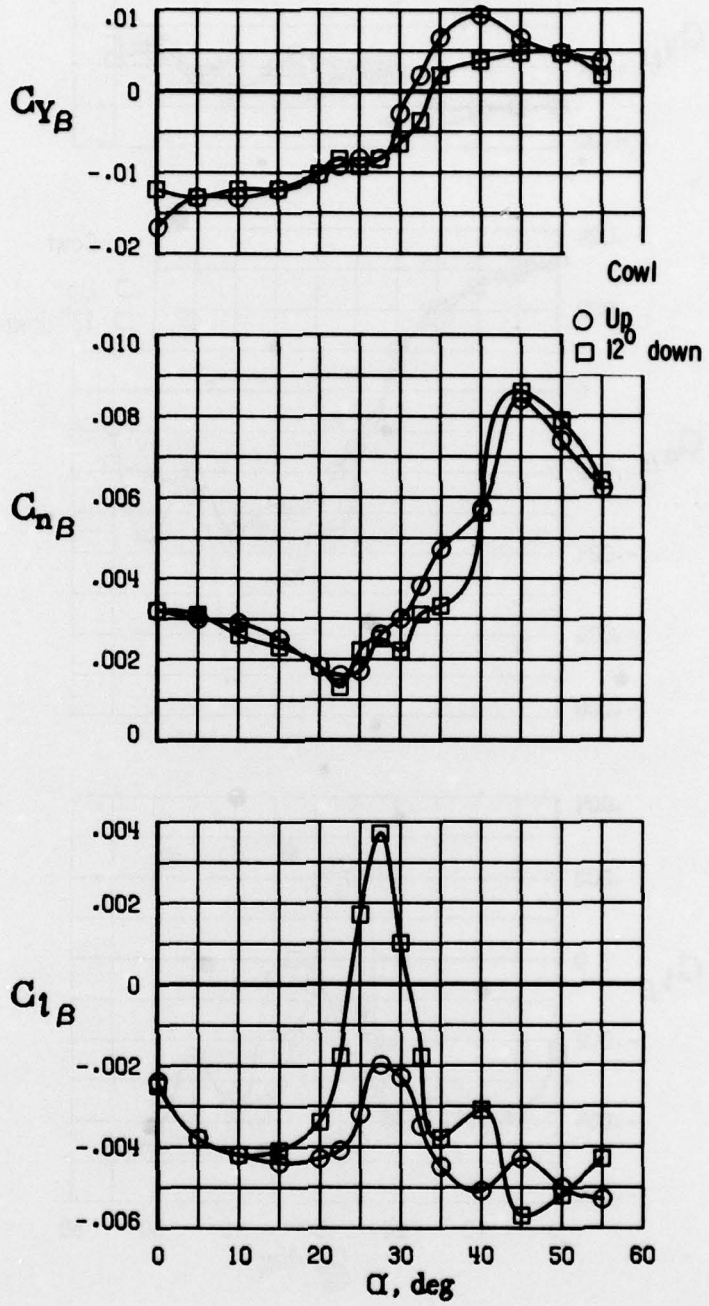

(b) 3.5 DKB forebody.

Figure 25.- Concluded.

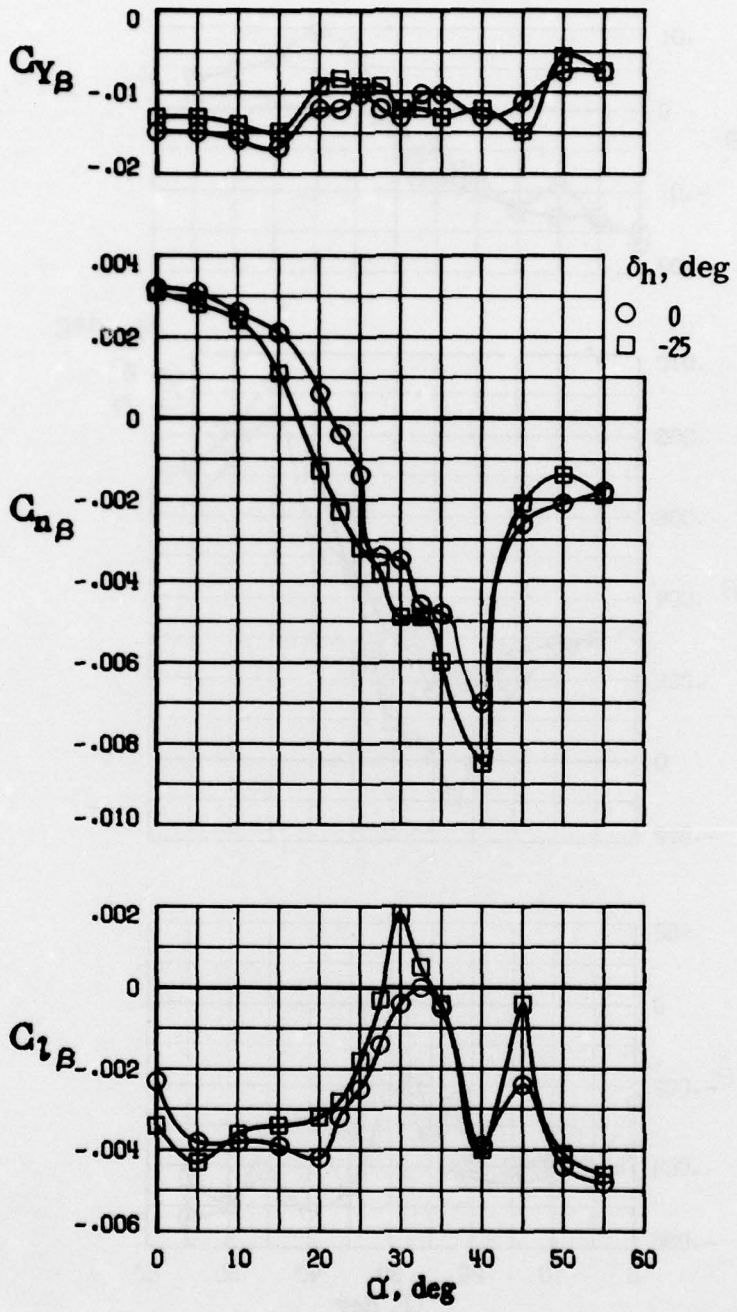

(a) 3.5 CIR forebody.

Figure 26.- Effect of horizontal-tail deflection on lateral-directional stability for two 3.5 fineness ratio forebodies; inlet cowl 12° down.

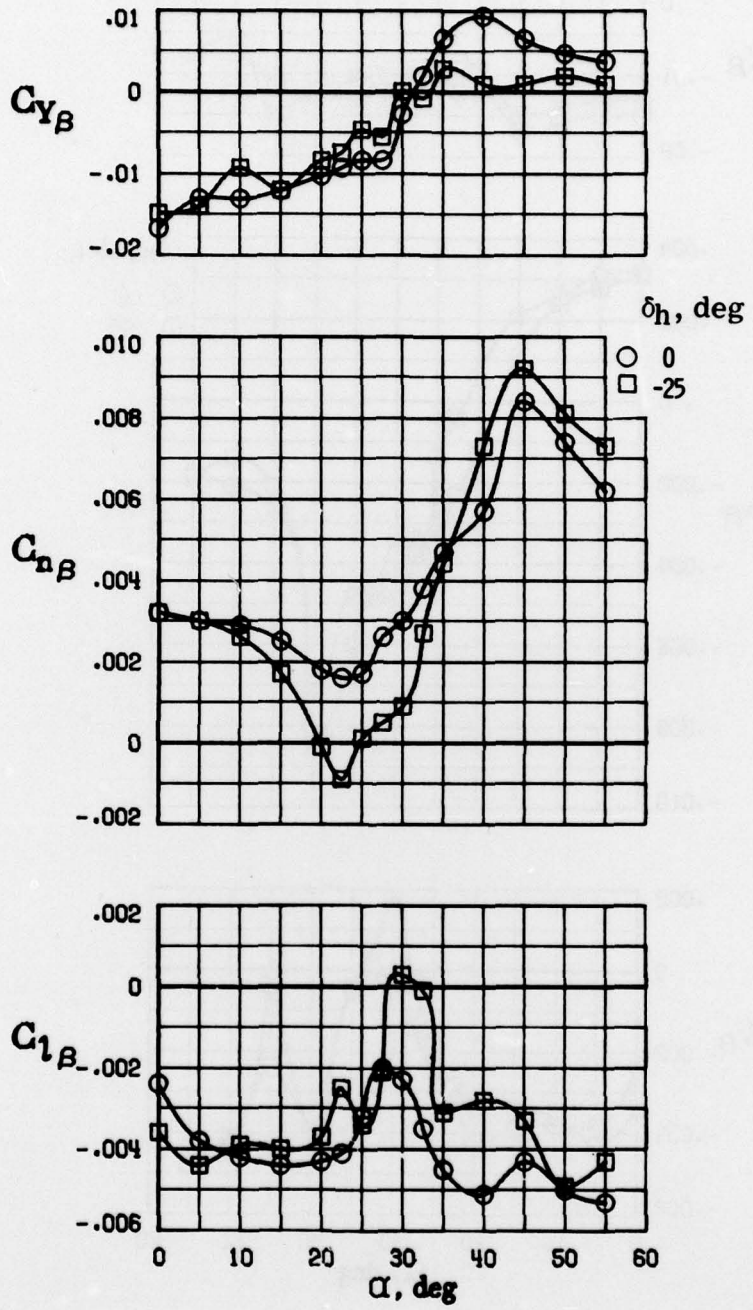

(b) 3.5 DKB forebody.

Figure 26.- Concluded.

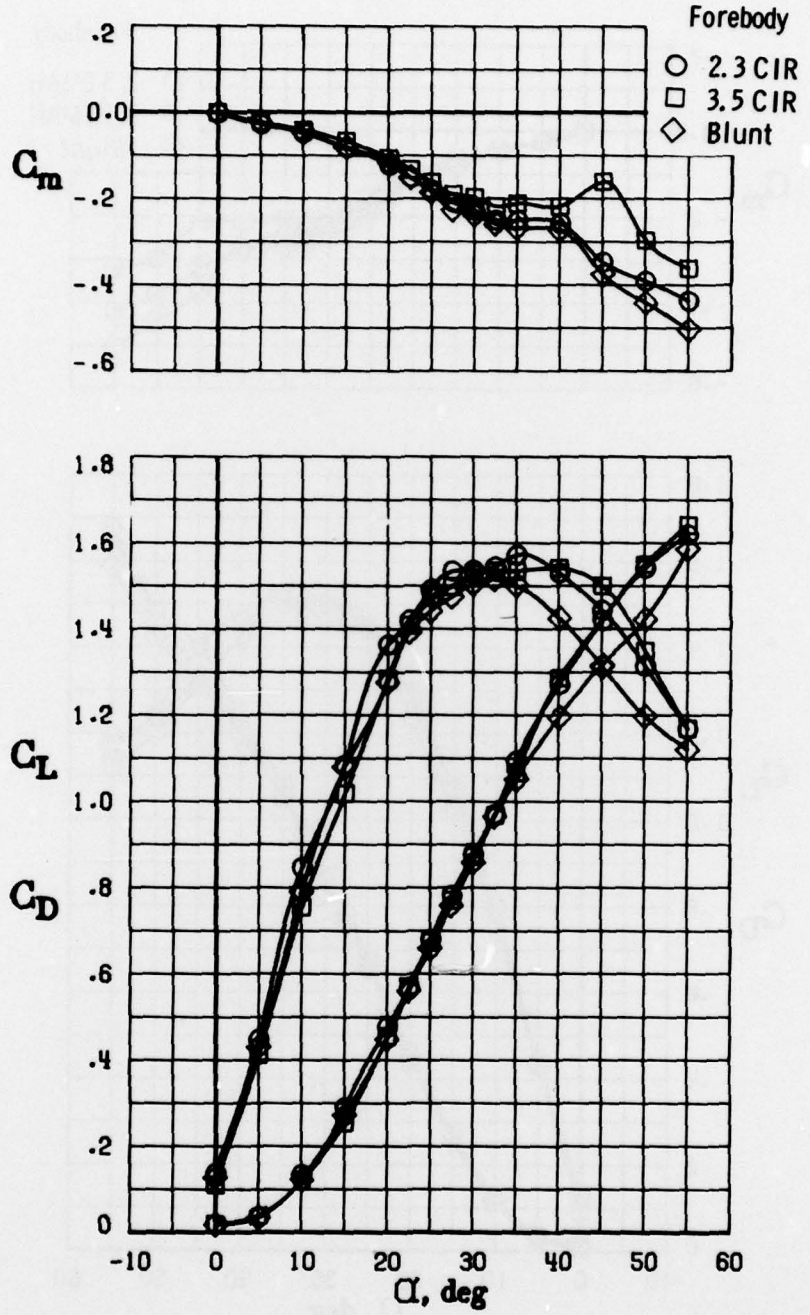

(a) CIR cross section.

Figure 27.- Effect of forebody fineness ratio on longitudinal characteristics; $\beta = 0^{\circ}$; $\delta_h = 0^{\circ}$; inlet cowl 12° down.

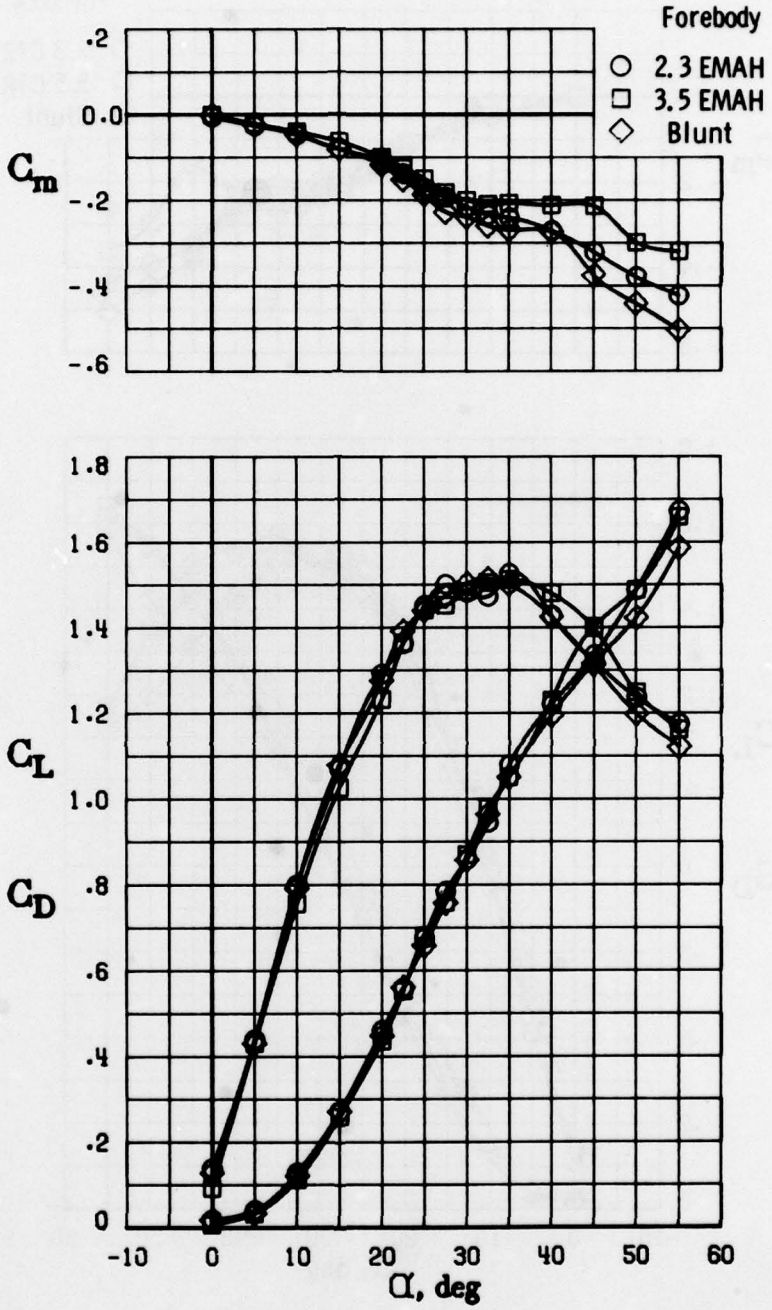

(b) EMAH cross section.

Figure 27.- Concluded.

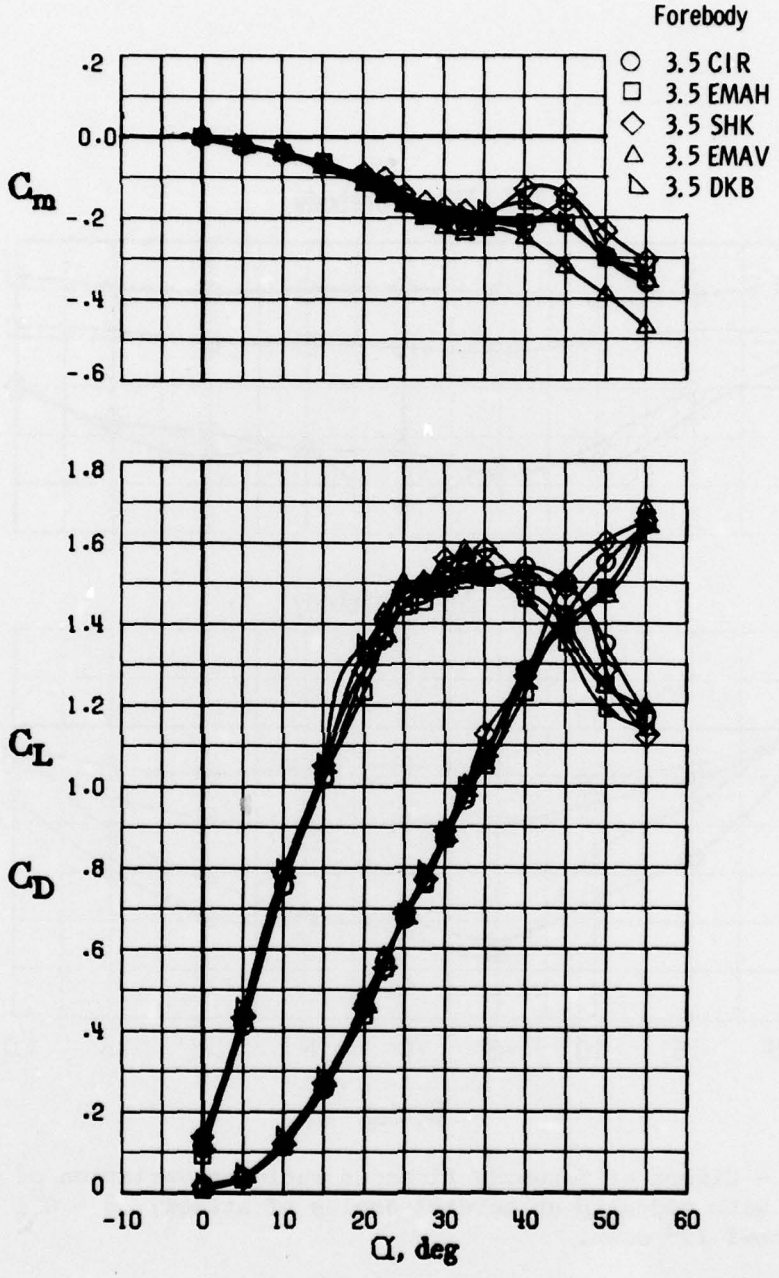

Figure 28.- Effect of forebody cross-sectional shape on longitudinal characteristics for 3.5 fineness ratio forebodies; $\beta = 0^\circ$; $\delta_h = 0^\circ$; inlet cowl 12° down.

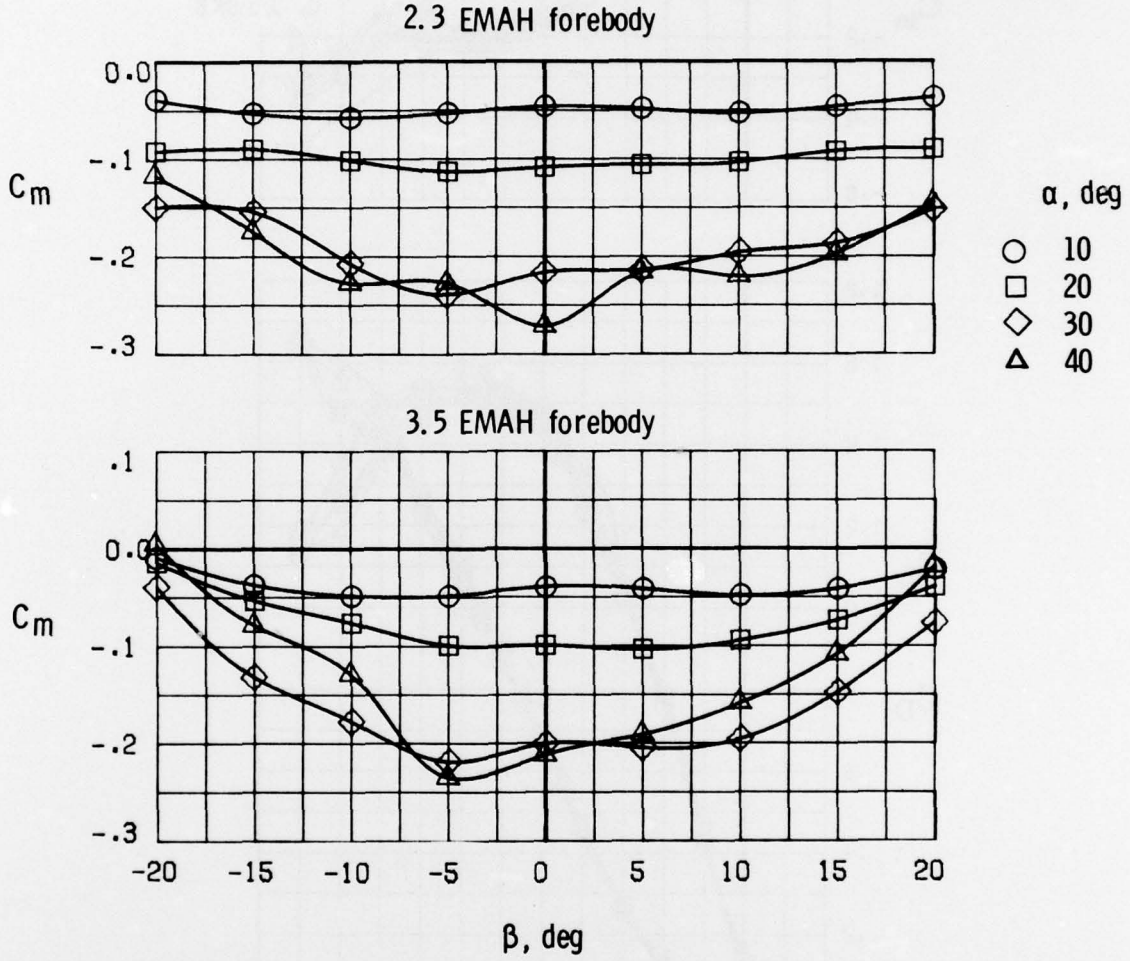

Figure 29.- Effect of forebody fineness ratio on variation of pitching moment with sideslip at several angles of attack; $\beta = 0^{\circ}$; $\delta_h = 0^{\circ}$; inlet cowl 12° down.

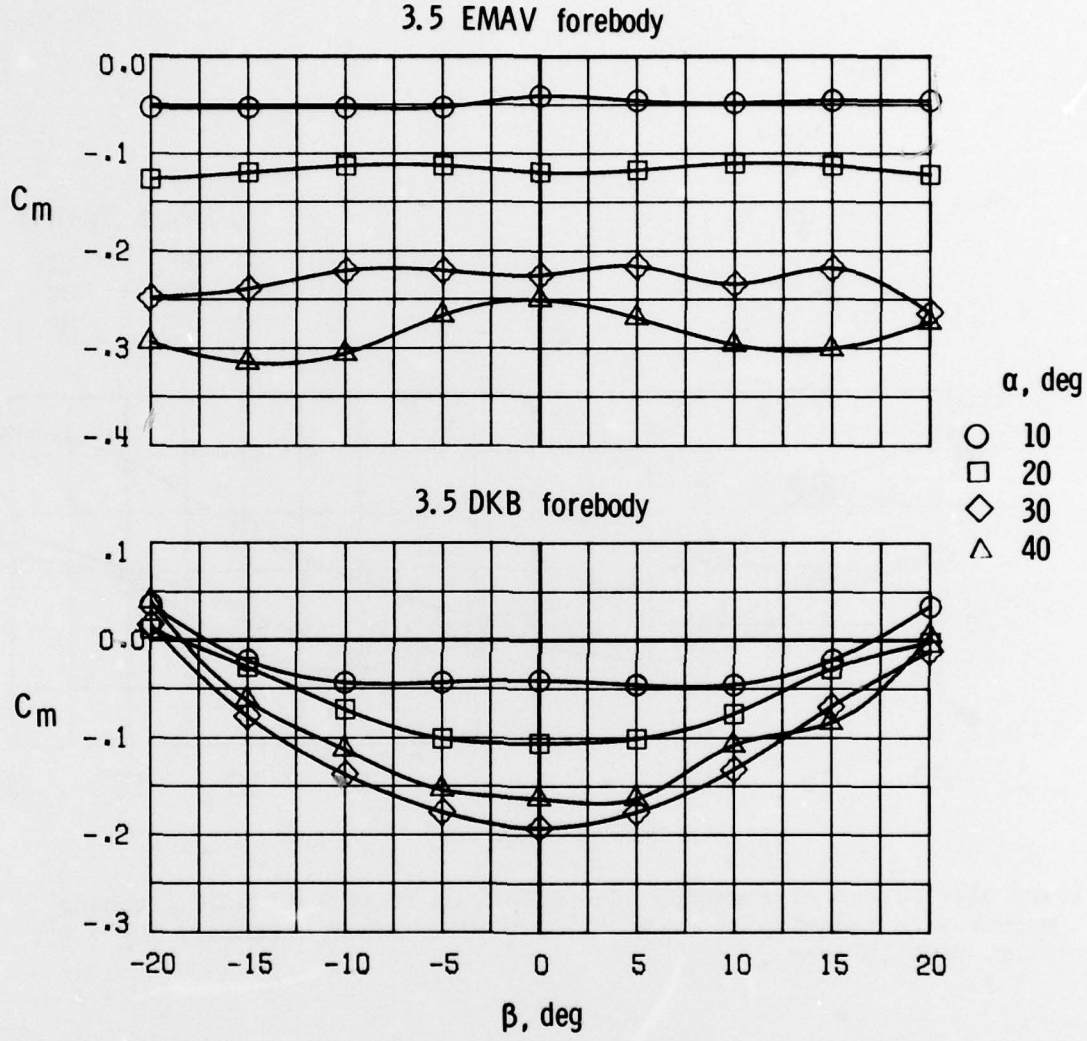

Figure 30.- Effect of forebody cross-sectional shape on variation of pitching moment with sideslip at several angles of attack; $\beta = 0^\circ$; 3.5 fineness ratio; $\delta_h = 0^\circ$; inlet cowl 12° down.

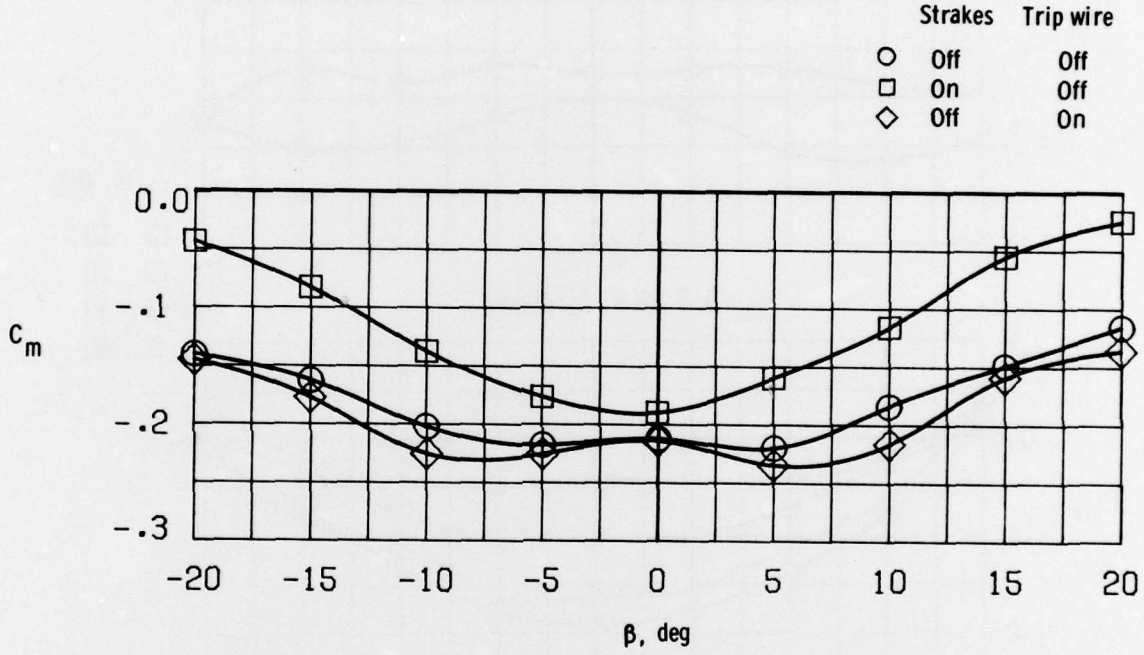

Figure 31.- Effect of forebody add-on devices on variation of pitching moment with sideslip at 32.5° α; β = 0°; 3.5 CIR forebody; δ_h = 0°; inlet cowl 12° down.

1. Report No.	2. Government Accession No.	3. Recipient's Catalog No.
NASA TP-1592		

4. Title and Subtitle	5. Report Date
EFFECTS OF FUSELAGE FOREBODY GEOMETRY ON LOW-SPEED LATERAL-DIRECTIONAL CHARACTERISTICS OF TWIN-TAIL FIGHTER MODEL AT HIGH ANGLES OF ATTACK	December 1979
	6. Performing Organization Code
7. Author(s)	8. Performing Organization Report No.
Peter C. Carr and William P. Gilbert	L-13270
	10. Work Unit No.
9. Performing Organization Name and Address	505-43-13-01
NASA Langley Research Center Hampton, VA 23665	11. Contract or Grant No.
	13. Type of Report and Period Covered
12. Sponsoring Agency Name and Address	Technical Paper
National Aeronautics and Space Administration Washington, DC 20546	14. Sponsoring Agency Code

15. Supplementary Notes

Peter C. Carr: Dryden Flight Research Center.
William P. Gilbert: Langley Research Center.

16. Abstract

Low-speed, static wind-tunnel tests have been conducted to explore the effects of fighter fuselage forebody geometry on lateral-directional characteristics at high angles of attack and to provide data for general design procedures. Effects of eight different forebody configurations and several add-on devices (e.g., nose strakes, boundary-layer trip wires, and nose booms) were investigated. Tests showed that forebody design features such as fineness ratio, cross-sectional shape, and add-on devices can have a significant influence on both lateral-directional and longitudinal aerodynamic stability. Several of the forebodies produced both lateral-directional symmetry and strong favorable changes in lateral-directional stability. However, the same results also indicated that such forebody designs can produce significant reductions in longitudinal stability near maximum lift and can significantly change the influence of other configuration variables. The addition of devices to highly tailored forebody designs also can significantly degrade the stability improvements provided by the clean forebody.

17. Key Words (Suggested by Author(s))	18. Distribution Statement
High angle of attack Aerodynamics Forebody effects Stability and control	Unclassified - Unlimited Subject Category 02

19. Security Classif. (of this report)	20. Security Classif. (of this page)	21. No. of Pages	22. Price*
Unclassified	Unclassified	70	$5.25

* For sale by the National Technical Information Service, Springfield, Virginia 22161

NASA-Langley, 1979

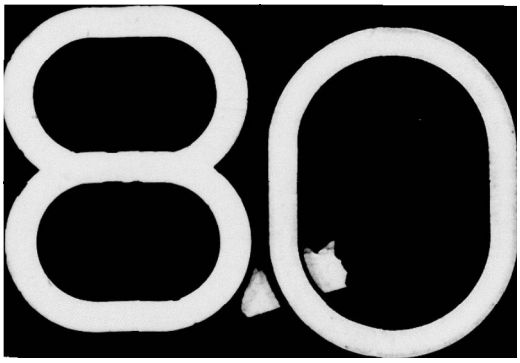
80